



# Measurement report: Molecular composition and volatility of gaseous organic compounds in a boreal forest – from volatile organic compounds to highly oxygenated organic molecules

Wei Huang<sup>1,★</sup>, Haiyan Li<sup>2,★</sup>, Nina Sarnela<sup>1</sup>, Liine Heikkinen<sup>1</sup>, Yee Jun Tham<sup>1</sup>, Jyri Mikkilä<sup>3</sup>, Steven J. Thomas<sup>1</sup>, Neil M. Donahue<sup>4</sup>, Markku Kulmala<sup>1</sup>, and Federico Bianchi<sup>1</sup>

<sup>1</sup>Institute for Atmospheric and Earth System Research/Physics, Faculty of Science, University of Helsinki, Helsinki, 00014, Finland

<sup>2</sup>School of Civil and Environmental Engineering, Harbin Institute of Technology, Shenzhen, 518055, China

<sup>3</sup>Karsa Oy., A. I. Virtasen aukio 1, Helsinki, 00560, Finland

<sup>4</sup>Center for Atmospheric Particle Studies, Carnegie Mellon University, 5000 Forbes Avenue, Pittsburgh, PA 15213, USA

★These authors contributed equally to this work.

**Correspondence:** Wei Huang (wei.huang@helsinki.fi) and Federico Bianchi (federico.bianchi@helsinki.fi)

Received: 10 December 2020 – Discussion started: 23 December 2020

Revised: 8 May 2021 – Accepted: 17 May 2021 – Published: 14 June 2021

**Abstract.** The molecular composition and volatility of gaseous organic compounds were investigated during April–July 2019 at the Station for Measuring Ecosystem – Atmosphere Relations (SMEAR) II situated in a boreal forest in Hyytiälä, southern Finland. In order to obtain a more complete picture and full understanding of the molecular composition and volatility of ambient gaseous organic compounds (from volatile organic compounds, VOCs, to highly oxygenated organic molecules, HOMs), two different instruments were used. A Vocus proton-transfer-reaction time-of-flight mass spectrometer (Vocus PTR-ToF; hereafter Vocus) was deployed to measure VOCs and less oxygenated VOCs (i.e., OVOCs). In addition, a multi-scheme chemical ionization inlet coupled to an atmospheric pressure interface time-of-flight mass spectrometer (MION API-ToF) was used to detect less oxygenated VOCs (using Br<sup>−</sup> as the reagent ion; hereafter MION-Br) and more oxygenated VOCs (including HOMs; using NO<sub>3</sub><sup>−</sup> as the reagent ion; hereafter MION-NO<sub>3</sub>). The comparison among different measurement techniques revealed that the highest elemental oxygen-to-carbon ratios (O:C) of organic compounds were observed by the MION-NO<sub>3</sub> (0.9 ± 0.1, average ± 1 standard deviation), followed by the MION-Br (0.8 ± 0.1); lowest O:C ratios were observed by Vocus (0.2 ± 0.1). Diurnal patterns of the measured organic compounds were found

to vary among different measurement techniques, even for compounds with the same molecular formula, suggesting contributions of different isomers detected by the different techniques and/or fragmentation from different parent compounds inside the instruments. Based on the complementary molecular information obtained from Vocus, MION-Br, and MION-NO<sub>3</sub>, a more complete picture of the bulk volatility of all measured organic compounds in this boreal forest was obtained. As expected, the VOC class was the most abundant (about 53.2 %), followed by intermediate-volatility organic compounds (IVOCs, about 45.9 %). Although condensable organic compounds (low-volatility organic compounds, LVOCs; extremely low volatility organic compounds, ELVOCs; and ultralow-volatility organic compounds, ULVOCs) only comprised about 0.2 % of the total gaseous organic compounds, they play an important role in new particle formation as shown in previous studies in this boreal forest. Our study shows the full characterization of the gaseous organic compounds in the boreal forest and the advantages of combining Vocus and MION API-ToF for measuring ambient organic compounds with different oxidation extents (from VOCs to HOMs). The results therefore provide a more comprehensive understanding of the molecular composition and volatility of atmospheric organic compounds as well as new insights into interpreting ambient measurements

or testing/improving parameterizations in transport and climate models.

## 1 Introduction

Organic aerosol (OA) has significant impacts on climate (IPCC, 2013), air quality (Boers et al., 2015), and human health (Nel, 2005; Rückerl et al., 2011). Large amounts of biogenic and anthropogenic volatile organic compounds (VOCs) are emitted into the atmosphere (Atkinson and Arey, 2003), with biogenic VOC (BVOC) emissions greatly surpassing anthropogenic VOC emissions globally (Heald et al., 2008). The global BVOC emissions are dominated by terpenes (isoprene ( $C_5H_8$ ),  $594 \text{ Tg C a}^{-1}$ ; monoterpenes ( $C_{10}H_{16}$ ),  $95 \text{ Tg C a}^{-1}$ ; and sesquiterpenes ( $C_{15}H_{24}$ ),  $20 \text{ Tg C a}^{-1}$ ) (Sindelarova et al., 2014), which are mainly emitted by vegetation and can be influenced by meteorological conditions, such as temperature and light (Guenther et al., 1995; Kaser et al., 2013). After being emitted, they can undergo gas-phase oxidation with ozone ( $O_3$ ), hydroxyl radical (OH), or nitrate radical ( $NO_3$ ), forming thousands of oxygenated VOCs (i.e., OVOCs) with diverse functionalities that can be grouped into different volatility classes: intermediate-volatility (IVOC), semi-volatile (SVOC), low-volatility (LVOC), extremely low volatility (ELVOC), and ultralow-volatility (ULVOC) organic compounds. Organic compounds with sufficiently low volatility (e.g., LVOCs, ELVOCs, and ULVOCs) can either form new particles or partition into the particle phase, contributing to particulate growth and mass (Ehn et al., 2014; Bianchi et al., 2016, 2019; Simon et al., 2020; Schervish and Donahue, 2020; Kulmala et al., 2013). Recent studies have shown that highly oxygenated organic molecules (HOMs; Bianchi et al., 2019) are a major source of condensing or nucleating compounds, and they play an important role in atmospheric new particle formation (Ehn et al., 2014; Bianchi et al., 2016; Kirkby et al., 2016; Tröstl et al., 2016; Bianchi et al., 2019; Kulmala et al., 1998). However, as a result of the complexity and analytical challenges of the precursor VOCs as well as the chemical composition and physicochemical properties of the resulting oxidation products (i.e., OVOCs), accurately predicting their effects on air quality and climate is still limited.

Mass spectrometric techniques represent one general approach to investigate the chemical composition of organic compounds (Sullivan and Prather, 2005; Nash et al., 2006). One common ionization technique used in aerosol research is chemical ionization (CI; e.g., Caldwell et al., 1989; Ehn et al., 2014; Lopez-Hilfiker et al., 2014; Huang et al., 2019a). It is a soft ionization method (Gross, 2017) that utilizes the reactivity of the analyte towards the reagent ion to ionize molecules via transfer of an electron, proton, or other ions such as bromide and nitrate (Caldwell et al., 1989; Ehn et al., 2014; Sanchez et al., 2016; Yuan et al., 2017; Krech-

mer et al., 2018). Different chemical ionization mass spectrometers (CIMSs) have different capabilities and sensitivities for detecting organic compounds (Riva et al., 2019). Proton-transfer-reaction mass spectrometry (PTR-MS) has been widely used to measure VOCs in the atmosphere (Yuan et al., 2017). The recently developed Vocus PTR time-of-flight mass spectrometer (Vocus PTR-ToF) has greatly enhanced sensitivity due to a newly designed chemical ionization source (Krechmer et al., 2018), and it can detect a broader spectrum of VOCs (even diterpenes) and their oxygenated products (up to six to eight oxygen atoms for monoterpene oxidation products; Li et al., 2020). However, Vocus PTR-ToF is not preferred for detecting HOMs or dimers (Li et al., 2020; Riva et al., 2019). The potential reason for the latter case could result from the fragmentation inside the instrument (Heinritzi et al., 2016) and/or losses in the sampling lines and on the walls of the inlet (Riva et al., 2019). The detection of less oxygenated VOCs (including less oxygenated dimers) and more oxygenated VOCs (including HOMs) can be well achieved by another instrument: an atmospheric pressure interface time-of-flight mass spectrometer (API-ToF) coupled to a novel chemical ionization inlet, Multi-scheme chemical IONization inlet (MION; Rissanen et al., 2019). Via the fast switching between multiple reagent ion schemes (i.e., bromide and nitrate), it has been found that MION API-ToF is able to provide a more complete picture of the OVOCs for laboratory experiments performed in flow tube reactors (Rissanen et al., 2019). Br-CIMS has been found to have similar or even higher sensitivities than that of iodide-CIMS towards OVOCs depending on humidity (Hyttinen et al., 2018). It has also been used for the detection of hydroperoxyl radicals (Sanchez et al., 2016) and peroxy radicals formed by autoxidation (Rissanen et al., 2019). In addition to the molecular composition of organic compounds itself provided by the abovementioned state-of-the-art instruments (i.e., Vocus PTR-ToF and MION API-ToF), this information can also be used in volatility parameterizations to calculate effective saturation mass concentrations ( $C_{\text{sat}}$ ) of individual organic compounds (Li et al., 2016; Donahue et al., 2011; Mohr et al., 2019), which can be then grouped into different volatility classes (or bins), i.e., volatility basis sets (VBSs; e.g., Donahue et al., 2006, 2011, 2012; Cappa and Jimenez, 2010). However, due to the different instrumental capabilities and sensitivities as well as the lack of calibration standards for the majority of organic compounds for the different measurement techniques as abovementioned, it still remains challenging to provide a comprehensive understanding of the molecular composition and volatility of both VOCs and OVOCs, particularly in the field.

In the present work, we investigate the chemical composition and volatility of gaseous organic compounds (VOCs and OVOCs) measured during April and July 2019 in a boreal forest in Hyytiälä, southern Finland. The capabilities of the recently developed MION API-ToF for measuring ambient

OVOCs are reported for the first time. Besides, the molecular composition and volatility of the OVOCs measured by MION API-ToF are compared and complemented with those OVOCs and their precursor VOCs observed with Vocus PTR-ToF. With the combination of the organic compounds measured by both instruments, we present a more comprehensive picture of the molecular composition and volatility of the gaseous organic compounds in this boreal forest.

## 2 Methodology

### 2.1 Site description

The measurements were conducted between 16 April–26 July 2019 at the University of Helsinki Station for Measuring Ecosystem – Atmosphere Relations (SMEAR) II (Hari and Kulmala, 2005), which is located in a boreal forest in Hyytiälä, southern Finland (61°51′N, 24°17′E; 181 m a.s.l.). This station is dominated by Scots pine (*Pinus sylvestris*), and monoterpenes are found to be the dominating emitted biogenic non-methane VOCs (Barreira et al., 2017; Hakola et al., 2012). The measurement station has been considered a rural background site (Manninen et al., 2010; Williams et al., 2011), and the nearest big city is Tampere, with more than 200 000 inhabitants and located ~60 km to the SW of our measurement site. A sawmill which is located 6–7 km away to the SE of our measurement site can contribute significantly to the OA loading in the case of SE winds, and the sawmill OA composition has been found to resemble biogenic OA a lot (Liao et al., 2011; Äijälä et al., 2017; Heikkinen et al., 2020).

### 2.2 Measurements, quantification, and volatility calculation of gaseous organic compounds

All mass spectrometers were set up in a temperature-controlled measurement container kept at ~25 °C. Sampling inlets were located about 1.5 m a.g.l. All data are reported in eastern European time (UTC+2).

#### 2.2.1 Measurements and quantification of gaseous organic compounds

An API-ToF (Tofwerk Ltd.; equipped with a long ToF with a mass resolving power of ~9000) coupled to a recently developed multi-scheme chemical ionization inlet (MION, Karsa Ltd.; Rissanen et al., 2019) was used to analyze the molecular composition of OVOCs at a time resolution of 30 min. During the 30 min cycles of measurements, MION API-ToF switched modes among nitrate ( $\text{NO}_3^-$ , 8 min), bromide ( $\text{Br}^-$ , 8 min), and API (measuring natural ions, 10 min) modes, followed by 2 min of ion-filter zeroing for the API mode before switching from API mode to the next mode. More details about the instrument are well described by Rissanen et al. (2019). Gaseous organic compounds were sampled via a

stainless-steel tube (1 in. outer diameter) of ca. 0.9 m length and a flow rate of  $20 \text{ L min}^{-1}$ . Due to the large inlet diameter and flow rate, the SVOC and HOM losses are expected to be insignificant. Through the fast switching between the two reagent ion schemes,  $\text{Br}^-$  and  $\text{NO}_3^-$ , less oxygenated VOCs (including less oxygenated dimers) and more oxygenated VOCs (including HOMs) can be measured, respectively (Rissanen et al., 2019). Data were analyzed with the software packages, “tofTools” (developed by Junninen et al., 2010) and “Labbis” (developed by Karsa Ltd.), which run in the MATLAB environment (MathWorks Inc., USA). Hereafter, results from these two reagent ion schemes are abbreviated as MION-Br and MION- $\text{NO}_3$ . The quantification of gaseous organic compounds measured with MION-Br and MION- $\text{NO}_3$  was calculated as in Eqs. (1) and (2), respectively:

$$[\text{org}] = \frac{\text{org}(\text{Br}^-)}{\text{Br}^- + \text{H}_2\text{O}(\text{Br}^-)} \times C_{\text{Br}^-}, \quad (1)$$

$$[\text{org}] = \frac{\text{org}(\text{NO}_3^-)}{\sum_{i=0}^2 (\text{HNO}_3^-)_i (\text{NO}_3^-)} \times C_{\text{NO}_3^-}, \quad (2)$$

where [org] is the concentration (unit:  $\text{cm}^{-3}$ ) of the gaseous organic compound (obtained from high-resolution fitting of each nominal mass) to be quantified; the numerators on the right-hand side are its detected signal clustered with bromide or nitrate, and the denominators are the sum of the reagent ion signals;  $C_{\text{Br}^-}$  and  $C_{\text{NO}_3^-}$  are the calibration factors representing the sensitivity of organic compound. The two stable isotopes of bromide ( $^{79}\text{Br}^-$  and  $^{81}\text{Br}^-$ ) share similar relative isotopic abundance, but only the compound clustered with  $^{79}\text{Br}^-$  was used for the quantification (Sanchez et al., 2016), as the calibration factor,  $C_{\text{Br}^-}$ , was also calculated in a similar way. Following the approach by Rissanen et al. (2019), the calibration factors  $C_{\text{Br}^-}$  and  $C_{\text{NO}_3^-}$  for sulfuric acid ( $\text{H}_2\text{SO}_4$ , compound representing the kinetic limit sensitivity; Viggiano et al., 1997; Berresheim et al., 2000) were determined to be  $2.33 \times 10^{11}$  and  $4.68 \times 10^{10} \text{ cm}^{-3}$ , respectively. The calibration factors are higher than those reported by Rissanen et al. (2019) due to different instrumental settings and inlet setup. By comparing the ambient  $\text{H}_2\text{SO}_4$  concentrations measured by MION-Br and MION- $\text{NO}_3$ , the median value (0.53) was used to scale down the  $\text{H}_2\text{SO}_4$  concentration measured by MION-Br, due to the fact that the high water vapor concentrations in the calibration kit ( $\sim 5 \times 10^{14-16} \text{ cm}^{-3}$ ) might cause some uncertainties in the  $\text{H}_2\text{SO}_4$  calibration factor of MION-Br (Hyttinen et al., 2018; Kürten et al., 2012). However, the MION-Br sensitivity has been found to be invariant with the measured ambient RH at our measurement site (20%–100%), e.g., for hydroperoxyl radicals (Sanchez et al., 2016), and the water clustered with  $\text{Br}^-$  has also been included in the signal normalization of organic compounds to account for the humidity

effect on reagent ion competition (see Eq. 1). With the maximum sensitivity applied, the concentrations therefore represent a lower limit. The uncertainties in the measured organic compound concentrations using calibration factors for H<sub>2</sub>SO<sub>4</sub> have been reported to be ±50 % (Ehn et al., 2014) or a factor of 2 (Berndt et al., 2015). However, the uncertainties could be higher with variations in, for example, temperature and relative humidity (RH) in the field.

A Vocus PTR-ToF (Aerodyne Research Inc.; hereafter Vocus) was deployed to measure VOCs and less oxygenated VOCs at a time resolution of 5 s. During the measurements, the Vocus ionization source was operated at a pressure of 1.5 mbar. The ambient air was sampled via a polytetrafluoroethylene (PTFE) tube of ca. 1 m length and a total sample flow of 4.5 L min<sup>-1</sup>. Of the total sample flow, around 100–150 cm<sup>3</sup> min<sup>-1</sup> went into the Vocus and the remainder was directed to the exhaust. The Vocus was automatically calibrated every 3 h using a multi-component standard cylinder. The standard gases were diluted by the injection of zero air with a built-in active carbon filter, producing the VOCs mixing ratio of around 5 ppb. The sensitivity of VOCs measured by PTR instruments has been shown to relate to their elemental composition and functionality (Sekimoto et al., 2017). Some compounds were calibrated using authentic standards, including isoprene, monoterpenes, and some aromatic compounds. Compounds without authentic standards were divided into four different molecular groups, the CH (compounds with only carbon and hydrogen atoms), CHO (compounds with only carbon, hydrogen, and oxygen atoms), CHON (compounds with only carbon, hydrogen, oxygen, and nitrogen atoms), and others. Compounds with the formula of CH and CHO were quantified with the average sensitivities of the standards CH and CHO, respectively. For the groups of CHON and others, there was no standard available in the calibration mixture. We used the average sensitivity of all the CH and CHO standards to quantify CHON compounds and others. Quantification using the relationship between the kinetic reaction rate constants and calibrated sensitivity (Sekimoto et al., 2017; Yuan et al., 2017) did not show huge differences (slopes between 0.59–0.75; see Fig. S1 in the Supplement) for the concentrations of several CH species (e.g., sesquiterpenes and diterpenes) or several dominant CHO and CHON species (e.g., C<sub>7</sub>H<sub>10</sub>O<sub>4</sub>, C<sub>8</sub>H<sub>12</sub>O<sub>4</sub>, and C<sub>10</sub>H<sub>15</sub>NO<sub>6–7</sub>) compared to the abovementioned quantification method we used. The Vocus data analysis was performed using the software package “Tofware” (provided by Tofwerk Ltd.) that runs in the Igor Pro environment (WaveMetrics Inc., USA). Signals were pre-averaged over 30 min before the analysis.

When combining the organic compounds measured by the three different ionization techniques (i.e., MION-Br, MION-NO<sub>3</sub>, and Vocus), for organic compounds observed in all ionization techniques, the highest concentration was used. Background subtraction was performed for all spectra; therefore, a lower signal for the same compound detected by any of the

ionization techniques suggests a lower ionization efficiency of the corresponding method (Stolzenburg et al., 2018).

## 2.2.2 Volatility calculation of gaseous organic compounds

Effective saturation mass concentration ( $C_{\text{sat}}$ ), a measure for volatility of a compound, was parameterized for each organic compound using the approach by Li et al. (2016) as in Eq. (3):

$$\log_{10} C_{\text{sat}}(298 \text{ K}) = \left( n_{\text{C}}^0 - n_{\text{C}} \right) b_{\text{C}} - n_{\text{O}} b_{\text{O}} - 2 \frac{n_{\text{C}} n_{\text{O}}}{(n_{\text{C}} + n_{\text{O}})} b_{\text{CO}} - n_{\text{N}} b_{\text{N}} - n_{\text{S}} b_{\text{S}}, \quad (3)$$

where  $n_{\text{C}}$ ,  $n_{\text{O}}$ ,  $n_{\text{N}}$ , and  $n_{\text{S}}$  are the number of carbon, oxygen, nitrogen, and sulfur atoms in the organic compound, respectively;  $n_{\text{C}}^0$  is the reference carbon number;  $b_{\text{C}}$ ,  $b_{\text{O}}$ ,  $b_{\text{N}}$ , and  $b_{\text{S}}$  are the contribution of each atom to  $\log_{10} C_{\text{sat}}$ , respectively; and  $b_{\text{CO}}$  is the carbon–oxygen nonideality (Donahue et al., 2011). These “ $b$ ” values depend on the composition of precursor gases, such as whether the precursors are aliphatic (including terpenes) or aromatic. In addition to being derived from literature structure–activity relations (i.e., SIMPOL; Pankow and Asher, 2008), the relations have been quantitatively confirmed for both aliphatic and aromatic systems using filter inlet for gases and aerosols (FIGAERO) thermal desorption CIMS measurements on carefully controlled precursor oxidation experiments at the CLOUD (Cosmics Leaving Outdoor Droplets) facility at CERN (European Organization for Nuclear Research) (Ye et al., 2019; Wang et al., 2020). For the boreal forest conditions in this work, we use the aliphatic (more volatile) parameterization, and these “ $b$ ” values can be found in Li et al. (2016). Due to the fact that the empirical approach by Li et al. (2016) was derived with very few organonitrates and could therefore lead to bias for the estimated vapor pressure (Isaacman-VanWertz and Aumont, 2021), we modified the  $C_{\text{sat}}(298 \text{ K})$  of CHON compounds by replacing all NO<sub>3</sub> groups with OH groups (Daumit et al., 2013).

To obtain the  $C_{\text{sat}}(T)$ , we adjusted the  $C_{\text{sat}}(298 \text{ K})$  (Donahue et al., 2011; Epstein et al., 2010) to the measured ambient temperature as in Eqs. (4) and (5):

$$\log_{10} C_{\text{sat}}(T) = \log_{10} C_{\text{sat}}(298 \text{ K}) + \frac{\Delta H_{\text{vap}}}{R \ln(10)} \times \left( \frac{1}{298} - \frac{1}{T} \right), \quad (4)$$

$$\Delta H_{\text{vap}} \left( \text{kJ mol}^{-1} \right) = -11 \cdot \log_{10} C_{\text{sat}}(298 \text{ K}) + 129, \quad (5)$$

where  $T$  is the temperature in kelvin;  $C_{\text{sat}}(298 \text{ K})$  is the saturation mass concentration at 298 K;  $\Delta H_{\text{vap}}$  is the vaporization enthalpy; and  $R$  is the gas constant (8.3143 J K<sup>-1</sup> mol<sup>-1</sup>).

Uncertainties arising from the potential presence of isomers is limited within this dataset, since they cannot be differentiated using the formula-based parameterization with the only input being the molecular composition. Accuracy to within 1 order of magnitude for terpene oxidation products has been confirmed by calibrated thermal desorption measurement (Wang et al., 2020) and by closure with size-resolved growth rate measurements at the CLOUD experiment (Stolzenburg et al., 2018). Besides, the fragmentation of organic compounds inside the instruments (e.g., Vocus) may also bias the  $C_{\text{sat}}$  results towards higher volatilities, resulting from the signal bias of parent ions towards lower values and of fragment ions towards higher values (Heinritzi et al., 2016).

### 2.3 Additional co-located measurements

The meteorological parameters were continuously monitored at this measurement site. Temperature was monitored with a Pt100 sensor (platinum resistance thermometer with a resistance of 100  $\Omega$  at 0  $^{\circ}\text{C}$ ) inside a ventilated custom-made radiation shield, while wind directions and wind speed were measured with a 2D ultrasonic anemometer (Adolf Thies GmbH & Co. KG), and the global radiation was measured with an EQ08 pyranometer (Carter-Scott Manufacturing Pty. Ltd.). The main wind direction above the canopy during the measurement period was southwest (see Fig. S2). The mixing ratios of ozone ( $\text{O}_3$ ) and nitrogen oxides ( $\text{NO}$  and  $\text{NO}_2$ ) were measured with an ultraviolet light absorption analyzer (TEI 49C, Thermo Fisher Scientific Inc.) and a chemiluminescence analyzer (TEI 42CTL, Thermo Fisher Scientific Inc.), respectively. The mixing ratios of sulfur dioxide ( $\text{SO}_2$ ) were measured with a fluorescence analyzer (TEI 43CTL, Thermo Fisher Scientific Inc.).

An aerosol chemical speciation monitor (ACSM; Aerodyne Research Inc.; Ng et al., 2011) was deployed to continuously measure the non-refractory sub-micrometer aerosol particle chemical composition. The ACSM, which contains a quadrupole mass spectrometer, provided unit-mass-resolution mass spectra every 30 min. This information was chemically speciated to organic, sulfate, nitrate, ammonium, and chloride concentrations by the ACSM analysis software. The mass concentrations of each species were calculated based on frequently conducted ionization efficiency calibrations. The data were corrected for collection efficiency, which was ca. 60 % during the measurement period. The sampling was conducted through a  $\text{PM}_{2.5}$  cyclone and a Nafion dryer (RH < 30 %) with a stainless-steel tube of ca. 3 m length and a flow rate of 3  $\text{L min}^{-1}$  (only 1.4  $\text{cm}^3 \text{s}^{-1}$  into the ACSM). The recorded data were analyzed using the ACSM local v. 1.6.0.3 toolkit (provided by Aerodyne Research Inc.) within the Igor Pro v. 6.37 (WaveMetrics Inc., USA). More details about ACSM operation and data processing can be found in Heikkinen et al. (2020).

## 3 Results and discussion

### 3.1 Overview of the measurements

Figure 1 shows the overview of the time series of meteorological parameters (temperature, global radiation, and wind direction and wind speed), trace gas concentrations ( $\text{SO}_2$ ,  $\text{O}_3$ ,  $\text{NO}$ , and  $\text{NO}_2$ ), and total gaseous organic compounds measured by MION-Br, MION- $\text{NO}_3$ , and Vocus, as well as total particulate organics measured by ACSM. Note that relatively long-lived compounds like ethanol, acetone, and acetic acid are excluded from Vocus data presented in this study in order to focus on compounds actively involved in the fast photochemistry (all excluded compounds are listed in Table S1, and the time series of total organic compound concentrations including them are shown in Fig. S3). As we can see from Fig. 1a, most of the measurement days had strong photochemical activities with ambient temperature exhibiting clear diurnal patterns ranging between  $-3$  and  $32$   $^{\circ}\text{C}$ . In general, the time series of the total organics (both gas phase and particle phase; see Fig. 1e–f) measured by MION-Br, MION- $\text{NO}_3$ , Vocus, and ACSM were similar during the measurement period. Elevated levels of total gaseous and particulate organics (e.g., 17–24 May and 7–10 June; see Fig. 1e–f) were observed on warmer days with strong global radiation and with the main wind direction coming from southeast (the direction of the sawmill, e.g., 17–24 May) or southwest (e.g., 7–10 June; see Fig. 1a–b). Besides, higher concentrations of oxidants of VOCs (such as  $\text{O}_3$ ) and/or anthropogenic pollutants (such as  $\text{SO}_2$  and  $\text{NO}_x$ ) also followed some of the elevated concentrations of gaseous and/or particulate organics (e.g., 19 April–3 May, 17–24 May, and 7–10 June; see Fig. 1c–d). The observations of the elevated organics could result from higher VOC emissions (e.g., terpenes, the typically observed VOCs; Li et al., 2021; Fig. S3) influenced by meteorological conditions (i.e., temperature and/or light; Guenther et al., 1995; Kaser et al., 2013), different air mass origins (e.g., terpene pollution from the sawmill in the case of SE winds; Liao et al., 2011; Äijälä et al., 2017; Heikkinen et al., 2020), and chemistry initiated by or related with different trace gases (Yan et al., 2016; Massoli et al., 2018; Huang et al., 2019b; Heikkinen et al., 2020). The results suggest the important roles that meteorological parameters, trace gases, and air masses play in the emission and oxidation reactions of organic compounds. Due to the soft ionization processes of organic molecules in the Vocus, MION-Br, and MION- $\text{NO}_3$ , the molecular composition of organic compounds was obtained. In the next section we will discuss the molecular composition of the gaseous organic compounds measured by Vocus, MION-Br, and MION- $\text{NO}_3$ .

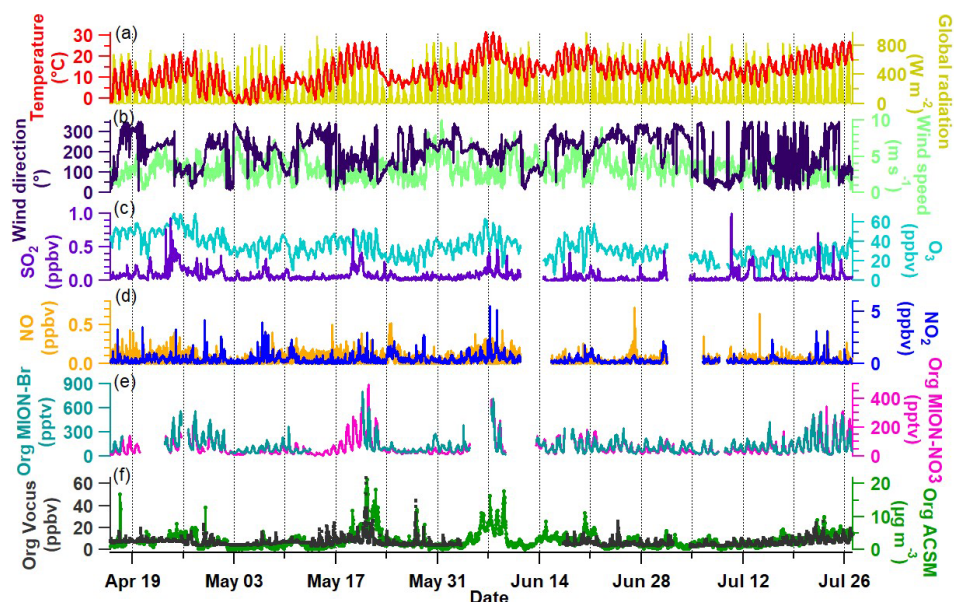


**Figure 1.** Overview of the time series from 16 April to 26 July 2019. (a) Temperature and global radiation; (b) wind direction and wind speed; (c) mixing ratios of SO<sub>2</sub> and O<sub>3</sub>; (d) mixing ratios of NO and NO<sub>2</sub>; (e) total gaseous organics measured by MION-Br and MION-NO<sub>3</sub>; and (f) total gaseous organics measured by Vocus as well as total particulate organics measured by ACSM. The data gap between MION-Br and MION-NO<sub>3</sub> (e.g., around 17 May) was due to the fact that the MION API-ToF was only running with API mode and NO<sub>3</sub> mode because of a mass flow controller issue for Br mode at that time.

### 3.2 Molecular composition of gaseous organic compounds

During the measurement period, Vocus identified 72 CH compounds ( $C_{x \geq 1}H_{y \geq 1}$ ) and 431 CHOX compounds ( $C_{x \geq 1}H_{y \geq 1}O_{z \geq 1}X_{0-n}$ ), with X being different atoms like N, S, or a combination thereof, while MION-Br and MION-NO<sub>3</sub> detected 567 and 687 CHOX compounds, respectively. Substantial overlaps of organic compounds were observed for these three ionization techniques, while distinct organic compounds were also detected with individual methods (Fig. S4). The average mass-weighted chemical compositions for organic compounds measured by Vocus, MION-Br, and MION-NO<sub>3</sub> were C<sub>5.3</sub>H<sub>7.5</sub>O<sub>1.1</sub>N<sub>0.1</sub>, C<sub>6.7</sub>H<sub>10.7</sub>O<sub>4.3</sub>N<sub>0.3</sub>, and C<sub>7.5</sub>H<sub>11.4</sub>O<sub>5.4</sub>N<sub>0.3</sub>, respectively. We stress here that the fragmentation of organic compounds inside the Vocus may bias the chemical composition towards a shorter carbon backbone. And the average mass-weighted chemical composition representing the bulk of all measured gaseous organic compounds (with the approach described in Sect. 2.2.1) in this boreal forest was calculated to be C<sub>6.0</sub>H<sub>8.7</sub>O<sub>1.2</sub>N<sub>0.1</sub>, indicative of the short carbon backbone and relatively low oxidation extent. Similar to previous laboratory results (Riva et al., 2019), MION-NO<sub>3</sub> observed the most oxidized compounds with the highest elemental oxygen-to-carbon ratios (O : C;  $0.9 \pm 0.1$ , average  $\pm 1$  standard deviation), followed by the MION-Br ( $0.8 \pm 0.1$ ); the O : C ratios of the organics detected by Vocus were lowest ( $0.2 \pm 0.1$ ). In addition, the CHO group comprised the largest fraction of the total organic

**Table 1.** Contribution (% , average  $\pm 1$  standard deviation) of different compound groups to total organics measured by different measurement techniques.

Compound group	Vocus	MION-Br	MION-NO <sub>3</sub>
CH	$35.2 \pm 15.1$ %	–	–
CHO	$43.6 \pm 9.4$ %	$75.4 \pm 5.3$ %	$71.8 \pm 7.9$ %
CHON	$8.1 \pm 2.7$ %	$24.1 \pm 5.2$ %	$28.1 \pm 7.9$ %
Others	$13.1 \pm 3.9$ %	$0.5 \pm 0.6$ %	$0.1 \pm 0.1$ %

compounds (Vocus:  $43.6 \pm 9.4$  %; MION-Br:  $75.4 \pm 5.3$  %; MION-NO<sub>3</sub>:  $71.8 \pm 7.9$  %; see Table 1). The second most abundant group for Vocus was the CH group, making up  $35.2 \pm 15.1$  % of its total organic compounds; while it was the CHON group for MION-Br ( $24.1 \pm 5.2$  %) and MION-NO<sub>3</sub> ( $28.1 \pm 7.9$  %; see Table 1), indicating active NO<sub>x</sub> or NO<sub>3</sub> radical-related chemistry (Yan et al., 2016). The CHON group only accounted for  $8.1 \pm 2.7$  % of the total organic compounds measured by Vocus, possibly due to its lower sensitivity towards larger organonitrates (see also Fig. S5) caused by their losses in the sampling lines and on the walls of the inlet (Riva et al., 2019) and/or fragmentation inside the instrument (Heinritzi et al., 2016).

The mass defect plots for organic compounds measured by Vocus, MION-Br, and MION-NO<sub>3</sub> are shown in Fig. 2. Similar to previous studies (e.g., Yan et al., 2016; Li et al., 2021), multiple series of organic compounds with different

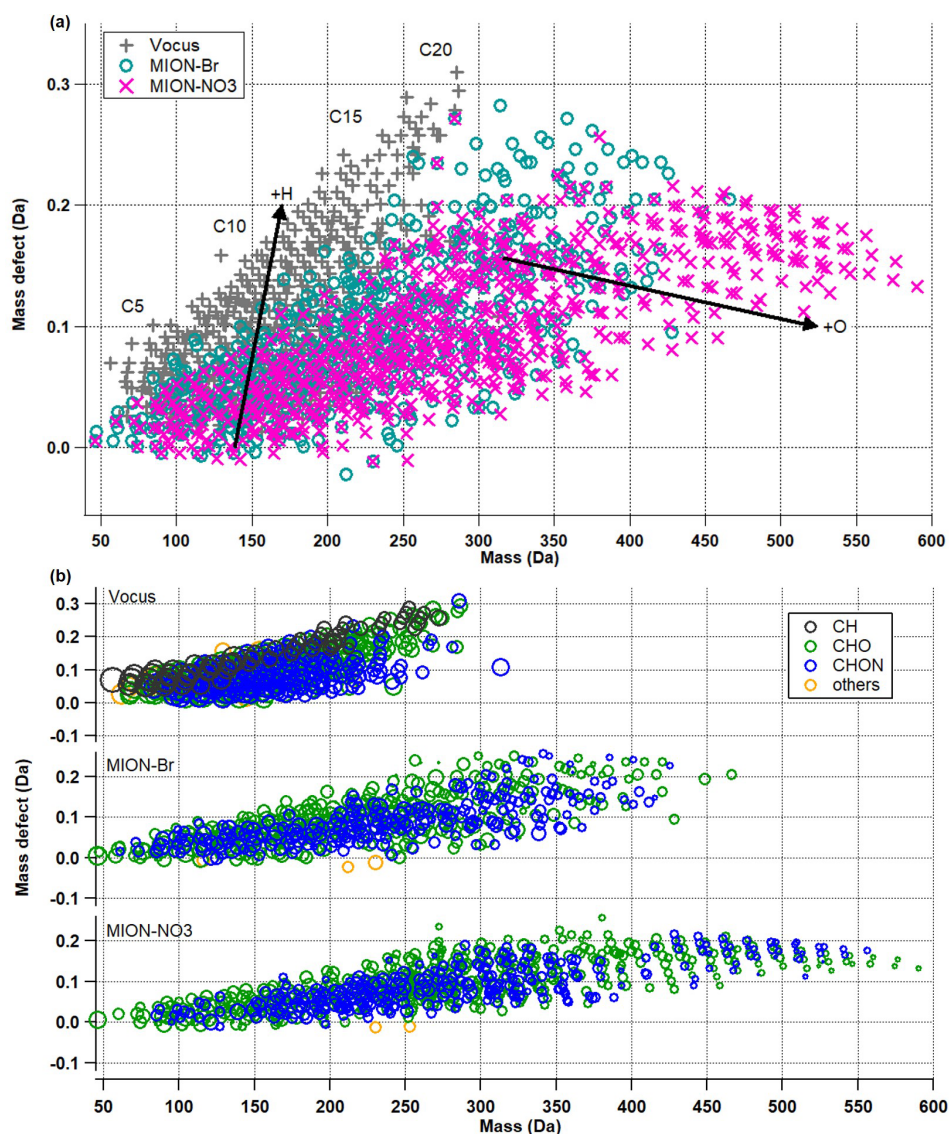


**Figure 2.** (a) Mass defect plots for organic compounds measured by Vocus, MION-Br, and MION-NO<sub>3</sub>; (b) mass defect plots for organic compounds (separated into CH, CHO, CHON, and others) measured by Vocus, MION-Br, and MION-NO<sub>3</sub>. Markers in panel (b) were all sized by the logarithm of their corresponding concentrations.

numbers of carbon atoms (such as C<sub>5</sub>, C<sub>10</sub>, C<sub>15</sub>, and C<sub>20</sub>) and oxygen atoms (up to 20; see also Fig. S5) were measured in this boreal forest environment. Organics with the lowest oxidation extent were better observed by Vocus, while organics with the largest molecular weights and highest oxidation extent were better observed by MION-NO<sub>3</sub> (Fig. 2a). Figure 2b shows the mass defect plots of organic compounds grouped into different categories. The markers are color-coded with different compound groups, such as CH, CHO, CHON, and others. The size of the markers is proportional to the logarithm of the concentration of each compound. Generally, similar to previous laboratory results (Riva et al., 2019; Rissanen et al., 2019), Vocus and MION-Br detected better the CHO compounds in the mass range of 50–100 Da and CHON

compounds in the mass range of 50–150 Da, and MION-Br even detected better the CHON compounds in the mass range of 350–425 Da, which are most likely to be less oxygenated monomers or dimers; MION-NO<sub>3</sub> was more sensitive towards the CHO and CHON compounds in the mass range of 425–600 Da, which are most likely to be more oxygenated HOM dimers (see Figs. 2b and S5).

We further investigated the contributions of the measured CHOX compounds with different numbers of oxygen atoms per molecule to total CHOX compounds as a function of the number of carbon atoms (Fig. 3). Organic compounds which were detected with higher sensitivity by Vocus were those with the number of carbon atoms between 3 and 10 and the number of oxygen atoms between 1 and 3 (i.e., less

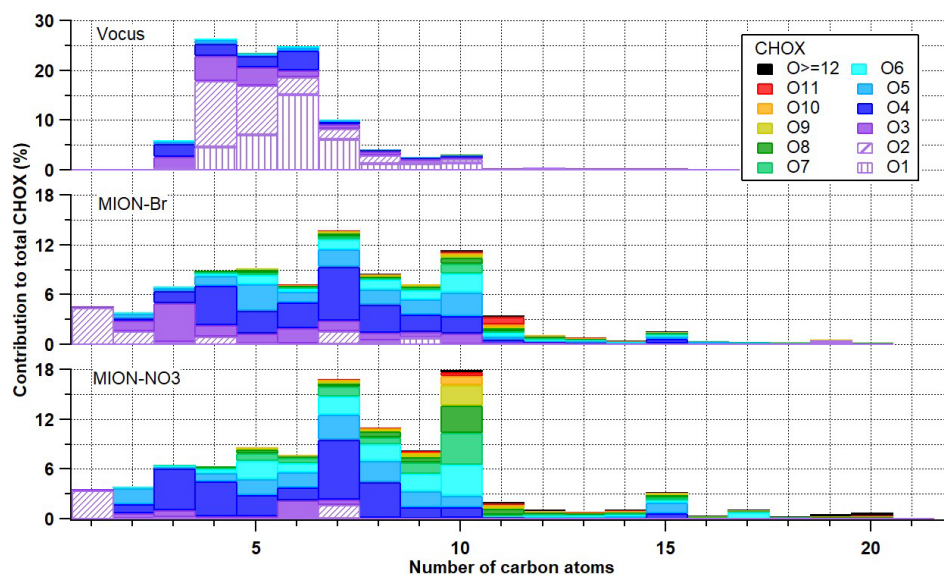


**Figure 3.** Contribution of measured CHOX compounds with different numbers of oxygen atoms to total CHOX compounds as a function of the number of carbon atoms for Vocus (a), MION-Br (b), and MION-NO<sub>3</sub> (c). Vocus panel has excluded CHX compounds (i.e., O<sub>0</sub> compounds).

oxygenated monomers). Compounds with a larger number of carbon atoms (i.e., > 10) and oxygen atoms (i.e., > 3) were much better detected by MION-Br and MION-NO<sub>3</sub>: the former particularly for CHON compounds with the number of carbon atoms between 15 and 20 and oxygen atoms between 4 and 8 (i.e., larger less oxygenated monomers and dimers; see Fig. S5b) and the latter particularly for compounds with the number of oxygen atoms larger than 9 (i.e., HOM monomers and dimers; Rissanen et al., 2019; Riva et al., 2019; Li et al., 2020; see Figs. 3 and S5). In the MION-Br and MION-NO<sub>3</sub> data, CHOX compounds with the number of carbon atoms of 5, 10, 15, and even 20 exhibited relatively elevated contributions compared to their neighbors (Fig. 3), indicating contributions of their potential corresponding precursors, i.e., isoprene, monoterpenes, sesquiterpenes, and diterpenes (together accounting for  $38.3 \pm 12.5\%$  of total CH compounds; see Table S2, Figs. S3, and S6). We emphasize here that using the number of carbon atoms as a basis to relate the CHOX to their precursor VOCs is a simplified assumption, as negative or positive artifacts can arise from fragmentation or accretion reactions (Lee et al., 2016). A similar pattern was also observed by Huang et al. (2019a) in a rural area in southwest Germany, based on filter inlet for gases and aerosols high-resolution time-of-flight chemical ionization mass spectrometer (FIGAERO-HR-ToF-CIMS) data. The consistency and complement of the results demonstrate the different capabilities of these instruments for measuring gaseous organic compounds with different oxidation extents (from VOCs to HOMs).

### 3.3 Diurnal characteristics of gaseous organic compounds

Median diurnal variations of total CH, total CHO, and total CHON compounds measured by Vocus, MION-Br, and MION-NO<sub>3</sub> are shown in Fig. 4. In general, the CH and CHO groups measured by Vocus exhibited higher levels during the night (see Fig. 4a–b), mainly driven by the boundary layer height dynamics (Baumbach and Vogt, 2003; Zha et al., 2018). Besides, CHO compounds measured by Vocus were dominated by O<sub>1–2</sub> compounds (see Figs. 3 and S5) and have also been reported to follow more the CH trends (Li et al., 2020). Their relatively flat diurnal pattern could result from the smearing effect after summing up the much less oxygenated CHO molecules (mostly peaking at night) and comparatively more oxygenated CHO molecules (mostly peaking during daytime) (Li et al., 2020). In contrast, the CHO and CHON groups measured by MION-Br and MION-NO<sub>3</sub> exhibited higher levels during the day (see Fig. 4b), due to strong photochemical oxidation caused by different meteorological parameters (i.e., temperature and global radiation; see Figs. 1a and S7), and/or elevated trace gas levels (e.g., O<sub>3</sub> and SO<sub>2</sub>; see Figs. 1c and S7; Yan et al., 2016; Masoli et al., 2018; Huang et al., 2019b; Bianchi et al., 2017). However, the CHON group measured by Vocus showed relatively stable signals throughout the day (see Fig. 4c). The potential reason could be partly due to its lower sensitivity towards larger organonitrates (see Fig. S5) caused by their losses in the sampling lines and on the walls of the inlet (Riva et al., 2019) and/or their fragmentation inside the instrument (Heinritzi et al., 2016). Another potential reason

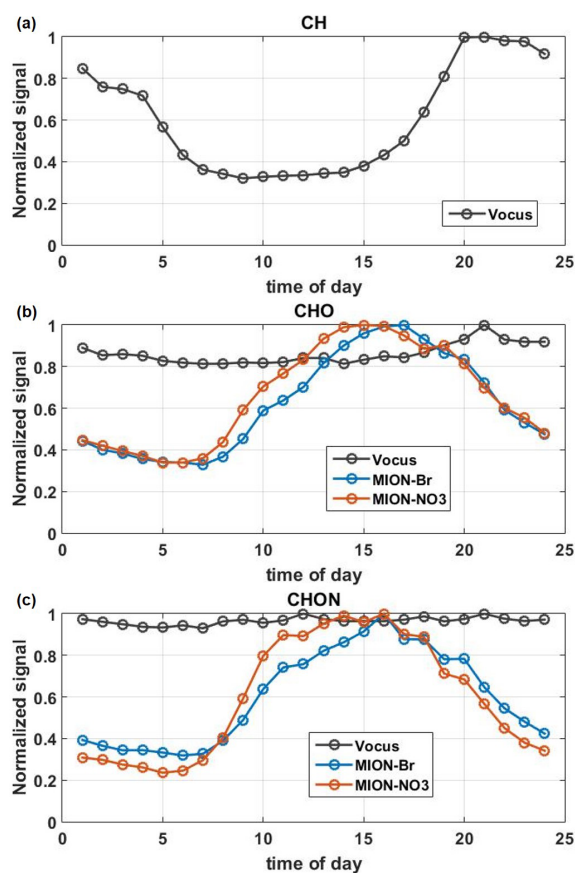


**Figure 4.** The median diurnal patterns of the total CH compounds measured by Vocus (a), CHO (b), and CHON compounds (c) measured by Vocus, MION-Br, and MION-NO<sub>3</sub> during the whole measurement period. Signals were normalized to their maximum values.

could result from the smearing effect after summing up the much less oxygenated CHON molecules (mostly peaking at night or early morning) and comparatively more oxygenated CHON molecules (mostly peaking during daytime) (Li et al., 2020).

Different diurnal patterns among different measurement techniques can also be found for individual organic compounds with the same molecular formula, such as several dominant CHO and CHON species, C<sub>7</sub>H<sub>10</sub>O<sub>4</sub> (molecular formula corresponding to 3,6-oxoheptanoic acid identified in the laboratory as limonene oxidation product by Faxon et al., 2018, and Hammes et al., 2019), C<sub>8</sub>H<sub>12</sub>O<sub>4</sub> (molecular formula corresponding to terpenylic acid identified in monoterpene oxidation product by Zhang et al., 2015, and Hammes et al., 2019), and C<sub>10</sub>H<sub>15</sub>NO<sub>6–7</sub> (identified in the laboratory as monoterpene oxidation products by Boyd et al., 2015, and Faxon et al., 2018; see Fig. 5). The inconsistent trends in time series and the varying correlations of these abovementioned dominant CHO and CHON species indicate different isomer contributions detected by different measurement techniques (Fig. S8 and Table S3). Similar behaviors were also evident

for OVOCs with varying oxidation extents, like the terpene-related C<sub>x</sub>HO and C<sub>x</sub>HON compounds ( $x = 5, 10, 15,$  and  $20$ ; see Fig. S9), which in total accounted for up to 27 % and 39 % of their corresponding CHO and CHON groups (see Table S2). Most of the terpene-related C<sub>x</sub>HO(N) groups ( $x = 5, 10, 15,$  and  $20$ ) with different oxidation extents behaved similarly among different measurement techniques, but some were also found to vary (see Fig. S9). Compounds with the same number of carbon and oxygen atoms but different numbers of hydrogen atoms (i.e., different saturation level) were also found to behave differently (see Fig. S9c–d), possibly due to different chemistry involved in their formation (Zhao et al., 2018; Molteni et al., 2019). Even compounds with the same molecular formula varied among different measurement techniques (see Fig. S9c–d and also Fig. 5). The differences can likely result from different isomers detected by the different techniques and/or fragmentation products from different parent compounds inside the instruments (e.g., Heinitz et al., 2016; Zhang et al., 2017).

The results indicate that organic compounds may behave differently among different measurement techniques during different time periods. In the next section, we will investigate the volatility of these gaseous organic compounds, which can influence their lifetime and roles in the atmosphere.

### 3.4 Volatility of organic compounds

Based on the log<sub>10</sub>C<sub>sat</sub> values of all organic compounds parameterized with the modified Li et al. (2016) approach (Daumit et al., 2013; Isaacman-VanWertz and Aumont, 2021) described in Sect. 2.2.2, the gaseous organic compounds were grouped into a 25-bin volatility basis set (VBS; Donahue et al., 2006) (Fig. 6a). Organic compounds with C<sub>sat</sub> lower than 10<sup>−8.5</sup> μg m<sup>−3</sup>, between 10<sup>−8.5</sup> and 10<sup>−4.5</sup> μg m<sup>−3</sup>, between 10<sup>−4.5</sup> and 10<sup>−0.5</sup> μg m<sup>−3</sup>, between 10<sup>−0.5</sup> and 10<sup>2.5</sup> μg m<sup>−3</sup>, between 10<sup>2.5</sup> and 10<sup>6.5</sup> μg m<sup>−3</sup>, and higher than 10<sup>6.5</sup> μg m<sup>−3</sup> are termed ULVOCs, ELVOCs, LVOCs, SVOCs, IVOCs, and VOCs, respectively (Donahue et al., 2009; Schervish and Donahue, 2020). The resulting VBS pie charts for these compound groups and their mean contributions are shown in Fig. 6b–d and Table 2. Organic compounds with C<sub>sat</sub> of 10<sup>4</sup> μg m<sup>−3</sup> made up the biggest mass contributions for MION-Br and MION-NO<sub>3</sub>, and the dominating C<sub>sat</sub> bin measured by Vocus was organic compounds with C<sub>sat</sub> of 10<sup>6</sup> μg m<sup>−3</sup> (see Fig. 6a). Furthermore, Vocus observed much higher contributions of VOCs with C<sub>sat</sub> higher than 10<sup>8</sup> μg m<sup>−3</sup>, whereas MION-NO<sub>3</sub> measured higher contributions of ELVOCs and ULVOCs with C<sub>sat</sub> lower than 10<sup>−8</sup> μg m<sup>−3</sup> (See Fig. 6a). And MION-Br and MION-NO<sub>3</sub> observed comparable contributions of compounds with C<sub>sat</sub> between 10<sup>−7</sup> and 10<sup>7</sup> μg m<sup>−3</sup>. We stress here that the fragmentation of organic compounds inside the Vocus may bias the C<sub>sat</sub> results towards higher volatilities.

IVOCs, which include generally less oxygenated VOCs, comprised the significant fraction of total organics (Vo-

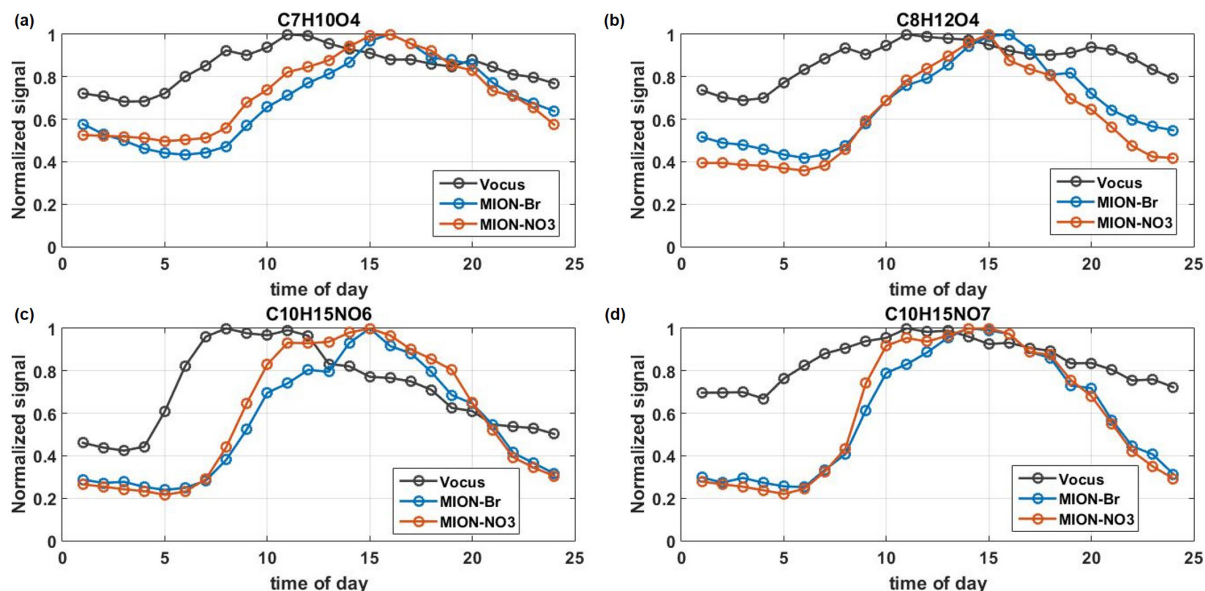


**Figure 5.** The median diurnal patterns of C<sub>7</sub>H<sub>10</sub>O<sub>4</sub> (a), C<sub>8</sub>H<sub>12</sub>O<sub>4</sub> (b), C<sub>10</sub>H<sub>15</sub>NO<sub>6</sub> (c), and C<sub>10</sub>H<sub>15</sub>NO<sub>7</sub> (d) measured by Vocus, MION-Br, and MION-NO<sub>3</sub> during the whole measurement period. Signals were normalized to their maximum values.

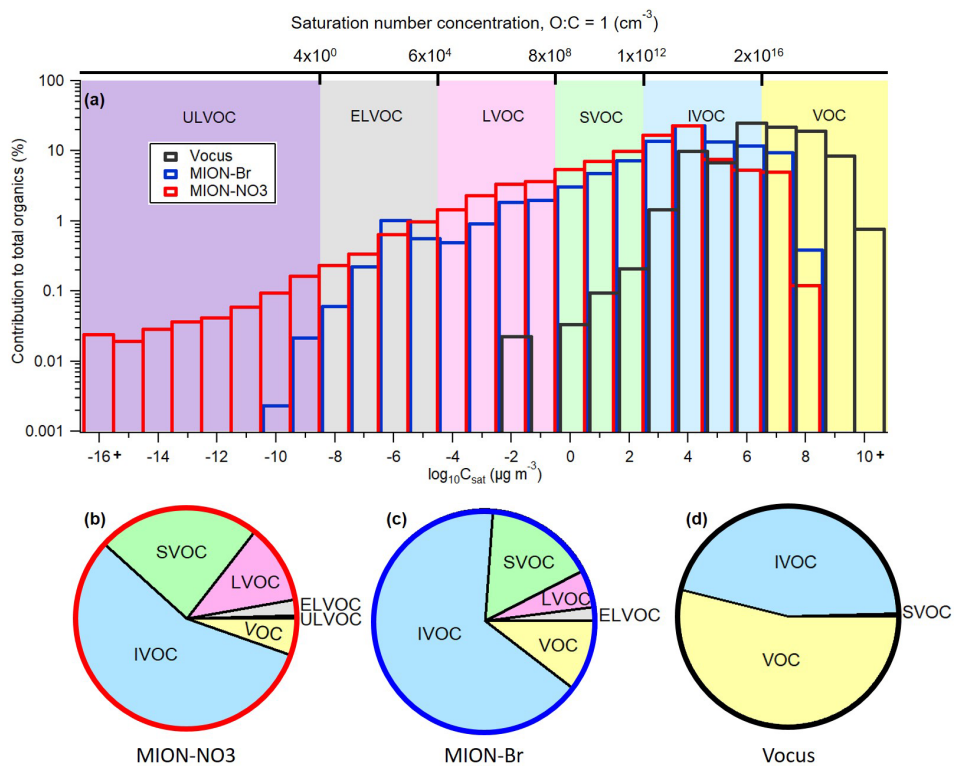


**Figure 6.** (a) Volatility distribution comparison for organic compounds detected by different measurement techniques and parameterized with the modified Li et al. (2016) approach (Daumit et al., 2013; Isaacman-VanWertz and Aumont, 2021); resulting pie charts for the contributions of VOC, IVOC, SVOC, LVOC, ELVOC, and ULVOC classes for MION-NO<sub>3</sub> (b); MION-Br (c); and Vocus (d). Contributions of LVOC for Vocus (0.02 ± 0.01 %) and ULVOC for MION-Br (0.02 ± 0.04 %) were not labeled in the pie chart.

**Table 2.** Contributions (% , average  $\pm 1$  standard deviation) of different compound groups to total organics measured by different measurement techniques based on the modified Li et al. (2016) approach (Daumit et al., 2013; Isaacman-VanWertz and Aumont, 2021).

Compound group	Vocus	MION-Br	MION-NO <sub>3</sub>
ULVOC	–	0.02 $\pm$ 0.04 %	0.5 $\pm$ 0.6 %
ELVOC	–	2.0 $\pm$ 1.8 %	2.3 $\pm$ 1.7 %
LVOC	0.02 $\pm$ 0.01 %	5.6 $\pm$ 2.9 %	11.6 $\pm$ 5.1 %
SVOC	0.4 $\pm$ 0.2 %	16.2 $\pm$ 4.9 %	23.9 $\pm$ 5.1 %
IVOC	45.8 $\pm$ 5.4 %	65.8 $\pm$ 8.5 %	56.3 $\pm$ 10.6 %
VOC	53.7 $\pm$ 5.5 %	10.4 $\pm$ 8.2 %	5.4 $\pm$ 2.4 %

cus: 45.8  $\pm$  5.4 %; MION-Br: 65.8  $\pm$  8.5 %; MION-NO<sub>3</sub>: 56.3  $\pm$  10.6 %), indicating substantial oxidation extent of the precursor VOCs, which made up 53.7  $\pm$  5.5 % of the total organics measured by Vocus but much less by MION-Br (10.4  $\pm$  8.2 %) and MION-NO<sub>3</sub> (5.4  $\pm$  2.4 %; see Fig. 6b–d and Table 2). SVOCs, which include slightly more oxygenated VOCs, constituted substantially (Vocus: 0.4  $\pm$  0.2 %; MION-Br: 16.2  $\pm$  4.9 %; MION-NO<sub>3</sub>: 23.9  $\pm$  5.1 %) to the measured organic compounds. LVOCs and ELVOCs, which include OVOCs with higher oxidation degrees and mainly contribute to the growth of embryonic clusters in the atmosphere (Donahue et al., 2012; Bianchi et al., 2019), accounted for > 8 % of the corresponding total organics measured by MION-Br and MION-NO<sub>3</sub>, while ULVOCs, which include OVOCs with even higher oxidation extents that are the most effective drivers of pure biogenic nucleation (Schervish and Donahue, 2020; Simon et al., 2020), accounted for 0.5  $\pm$  0.6 % of total organics measured by MION-NO<sub>3</sub> (see Fig. 6b–d and Table 2). Differences in the contribution of these compound groups (Fig. 6b–d and Table 2) could be due to different sensitivities of the instruments towards organic compounds with varying oxidation extents (Riva et al., 2019).

With the complementary molecular information of organic compounds from Vocus, MION-Br, and MION-NO<sub>3</sub>, a combined volatility distribution was plotted to estimate the bulk volatility of all measured organic compounds (with the approach described in Sect. 2.2.1) at our measurement site (Fig. 7). The combined volatility distribution covers very well from VOCs to HOMs, with varying O : C ratios and volatility ranges (Fig. 7a). It therefore provides a more complete picture of the volatility distribution of gaseous organic compounds in this boreal forest. The average mass-weighted log<sub>10</sub>C<sub>sat</sub> value representing the bulk of all measured gaseous organic compounds in this boreal forest was  $\sim 6.1 \mu\text{g m}^{-3}$ . In general, MION-NO<sub>3</sub> measured > 91 % of the ULVOCs, while MION-Br measured > 70 % of the ELVOCs and Vocus measured > 98 % of the IVOCs and VOCs (Fig. S10). As we can see from Fig. 7b, the VOC class was found to be the

most abundant (about 53.2 %), followed by the IVOC class (about 45.9 %), indicating that the bulk gaseous organic compounds observed in this boreal forest were relatively fresh, which is also consistent with the bulk molecular composition's relatively low oxidation extent. Differences in the bulk volatility of organic compounds between daytime (between 10:00 and 17:00) and nighttime (between 22:00 and 05:00) were not significant (Fig. S11). Given the location of the measurement station that is inside a boreal forested area, the gaseous organic compounds were expected to be dominated by VOCs and IVOCs. The abundance of the CH compounds such as terpenes (see Tables 1 and S2, Figs. S3 and S6) as well as less oxygenated VOCs (see Figs. 3 and S5) supports this conclusion. Although the condensable vapors (LVOCs, ELVOCs, and ULVOCs) only comprised about 0.2 % of the total gaseous organic compounds, they contribute significantly to forming new particles via nucleation and further particulate growth and mass via condensation in this boreal forest (Kulmala et al., 2013; Ehn et al., 2014; Mohr et al., 2019). The results from the combined VBS could provide a better basis to test and improve parameterizations for predicting organic compound evolutions in transport and climate models.

#### 4 Conclusions

In this paper, with an aim of obtaining a more complete picture from VOCs to HOMs, the molecular composition and volatility of gaseous organic compounds were investigated with the deployment of a Vocus and a MION API-ToF during April–July 2019 at the SMEAR II station situated in a boreal forest in Hyytiälä, southern Finland. Similar to previous laboratory results (Riva et al., 2019), highest elemental O : C ratios of organic compounds were observed by the MION-NO<sub>3</sub> (0.9  $\pm$  0.1), followed by the MION-Br (0.8  $\pm$  0.1), and lowest by the Vocus (0.2  $\pm$  0.1). Unlike the patterns observed by Vocus, which were mostly dominated by compounds with the number of carbon atoms between 3 and 10 and the number of oxygen atoms between 1 and 3 (i.e., less oxygenated monomers), compounds with a larger number of carbon atoms (i.e., > 10) and oxygen atoms (i.e., > 3) were much better detected by MION-Br (particularly for larger less oxygenated monomers and dimers) and MION-NO<sub>3</sub> (particularly for HOM monomers and dimers). The average mass-weighted chemical composition representing the bulk of all measured gaseous organic compounds in this boreal forest was C<sub>6,0</sub>H<sub>8,7</sub>O<sub>1,2</sub>N<sub>0,1</sub>, indicative of the short carbon backbone and relatively low oxidation extent. Besides, diurnal patterns of the measured organic compounds were found to vary among different measurement techniques, even for compounds with the same molecular formula. The results indicate contributions of different isomers detected by the different techniques and/or fragmentation products from dif-

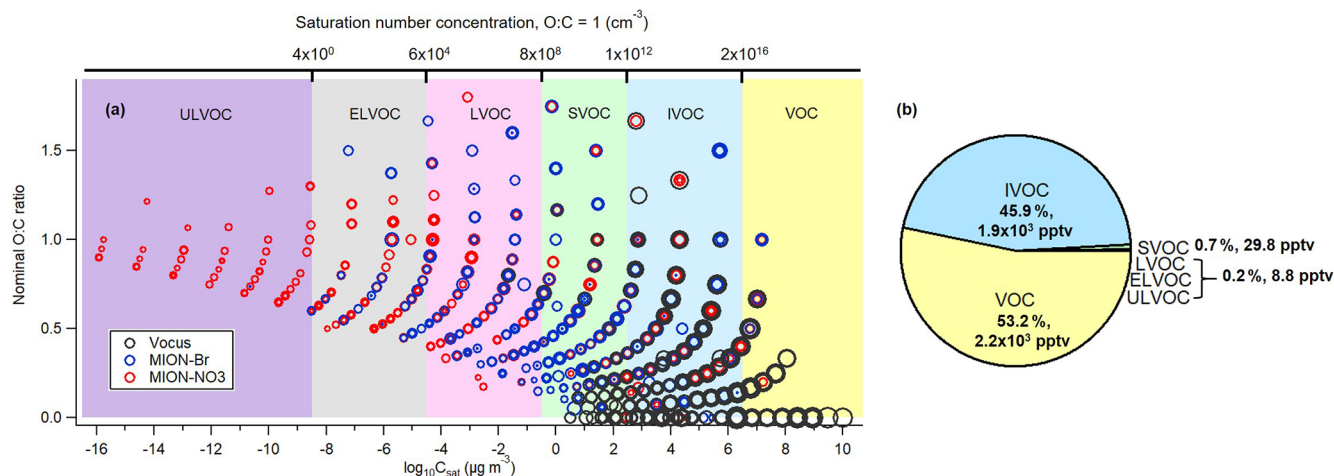


**Figure 7.** (a) Combined two-dimensional volatility distribution for all measured organic compounds (with the approach described in Sect. 2.2.1) parameterized with the modified Li et al. (2016) approach (Daumit et al., 2013; Isaacman-VanWertz and Aumont, 2021). Markers were sized by the logarithm of their corresponding concentrations, and marker color represents that either the compound was only measured by that instrument or the maximum concentration of the compound observed in common was detected by that instrument; (b) resulting pie chart for the contributions of VOC, IVOC, SVOC, LVOC, ELVOC, and ULVOC classes.

ferent parent compounds inside the instruments (e.g., Heintz et al., 2016; Zhang et al., 2017).

From the more complete picture of the bulk volatility of all measured organic compounds in this boreal forest, the average mass-weighted log<sub>10</sub>C<sub>sat</sub> value representing the bulk of all measured gaseous organic compounds in this boreal forest was  $\sim 6.1 \mu\text{g m}^{-3}$ . In addition, the VOC class was found to be the most abundant (about 53.2%), followed by the IVOC class (about 45.9%), indicating that the bulk gaseous organic compounds were relatively fresh, which is consistent with the bulk molecular composition's relatively low oxidation extent. Although condensable organic compounds (LVOCs, ELVOCs, and ULVOCs) only comprised about 0.2% of the total gaseous organic compounds, they play an important role, forming new particles via nucleation and contributing to particulate growth and mass via condensation in this boreal forest (Kulmala et al., 2013; Ehn et al., 2014; Mohr et al., 2019).

The results show the full characterization of the gaseous organic compounds in the boreal forest and the advantages of combining Vocus and MION API-ToF for measuring ambient gaseous organic compounds with different oxidation extents (from VOCs to HOMs). Our study provides a more comprehensive understanding of the molecular composition and volatility of atmospheric organic compounds, as well as new insights when interpreting ambient measurements or using them as input to test and improve parameterizations for predicting organic compound evolutions in transport and climate models.

**Data availability.** The time series of the measured trace gases, meteorological parameters, and the concentrations of terpenes (isoprene, monoterpenes, sesquiterpenes, and diterpenes measured by Vocus) as well as total organics (measured by MION-Br, MION-NO<sub>3</sub>, Vocus, and ACSM) at the SMEAR II station are available from <https://doi.org/10.5281/zenodo.4925730> (Huang, 2021).

**Supplement.** The supplement related to this article is available online at: <https://doi.org/10.5194/acp-21-8961-2021-supplement>.

**Author contributions.** WH analyzed the MION API-ToF data, produced all figures, and wrote and edited the paper. HL operated and calibrated Vocus; analyzed the Vocus data; provided suggestions for the data analysis, interpretation, and discussion; and edited the paper. NS operated and calibrated the MION API-ToF; preprocessed the MION API-ToF data with Labbis; and provided suggestions for the data analysis, interpretation, and discussion. LH performed ACSM measurements, analyzed the ACSM data, and provided suggestions for the data interpretation and discussion. YJT provided suggestions for the data interpretation and discussion. JM helped with the MION measurements and provided suggestions for the data interpretation and discussion. SJT helped with the Vocus measurements. NMD provided suggestions for the data interpretation and discussion. MK organized the campaign and provided suggestions for the data interpretation and discussion. FB organized the campaign; provided suggestions for the data analysis, interpretation, and discussion; and edited the paper. All authors contributed to the final text.

**Competing interests.** The authors declare that they have no conflict of interest.

**Acknowledgements.** This work was supported by the staff at INAR. Hyytiälä personnel are acknowledged for their help in conducting the measurements. Jani Hakala is acknowledged for his help with MION measurements. Junning Ma is acknowledged for his technical help with data analysis. We thank the tofTools team and Karsa Labbis team for providing tools for mass spectrometry data analysis.

**Financial support.** This research has been supported by the Academy of Finland (grant no. 311932), H2020 European Research Council (CHAPAs (grant no. 850614) and ATM-GTP (grant no. 742206)), Jane and Aatos Erkkö Foundation, and the National Science Foundation (grant no. AGS1801897).

Open-access funding was provided by the Helsinki University Library.

**Review statement.** This paper was edited by Eleanor Browne and reviewed by two anonymous referees.

## References

- Äijälä, M., Heikkinen, L., Fröhlich, R., Canonaco, F., Prévôt, A. S. H., Junninen, H., Petäjä, T., Kulmala, M., Worsnop, D., and Ehn, M.: Resolving anthropogenic aerosol pollution types – deconvolution and exploratory classification of pollution events, *Atmos. Chem. Phys.*, 17, 3165–3197, <https://doi.org/10.5194/acp-17-3165-2017>, 2017.
- Atkinson, R. and Arey, J.: Atmospheric degradation of volatile organic compounds, *Chem. Rev.*, 103, 4605–4638, <https://doi.org/10.1021/cr0206420>, 2003.
- Barreira, L. M. F., Duporte, G., Parshintsev, J., Hartonen, K., Jusila, M., Aalto, J., Back, J., Kulmala, M., and Riekkola, M. L.: Emissions of biogenic volatile organic compounds from the boreal forest floor and understory: a study by solid-phase microextraction and portable gas chromatography-mass spectrometry, *Boreal Environ. Res.*, 22, 393–413, 2017.
- Baumbach, G. and Vogt, U.: Influence of inversion layers on the distribution of air pollutants in urban areas, *Water Air Soil Poll.: Focus*, 3, 67–78, <https://doi.org/10.1023/A:1026098305581>, 2003.
- Berresheim, H., Elste, T., Plass-Dülmer, C., Eisele, F. L., and Tanner, D. J.: Chemical ionization mass spectrometer for long-term measurements of atmospheric OH and H<sub>2</sub>SO<sub>4</sub>, *Int. J. Mass Spectrom.*, 202, 91–109, [https://doi.org/10.1016/S1387-3806\(00\)00233-5](https://doi.org/10.1016/S1387-3806(00)00233-5), 2000.
- Berndt, T., Richters, S., Kaethner, R., Voigtlander, J., Stratmann, F., Sipilä, M., Kulmala, M., and Herrmann, H.: Gas-phase ozonolysis of cycloalkenes: formation of highly oxidized RO<sub>2</sub> radicals and their reactions with NO, NO<sub>2</sub>, SO<sub>2</sub>, and other RO<sub>2</sub> radicals, *J. Phys. Chem. A*, 119, 10336–10348, <https://doi.org/10.1021/acs.jpca.5b07295>, 2015.
- Bianchi, F., Tröstl, J., Junninen, H., Frege, C., Henne, S., Hoyle, C. R., Molteni, U., Herrmann, E., Adamov, A., Bukowiecki, N., Chen, X., Duplissy, J., Gysel, M., Hutterli, M., Kangasluoma, J., Kontkanen, J., Kürten, A., Manninen, H. E., Münch, S., Peräkylä, O., Petäjä, T., Rondo, L., Williamson, C., Weingartner, E., Curtius, J., Worsnop, D. R., Kulmala, M., Dommen, J., and Baltensperger, U.: New particle formation in the free troposphere: a question of chemistry and timing, *Science*, 352, 1109–1112, <https://doi.org/10.1126/science.aad5456> 2016.
- Bianchi, F., Garmash, O., He, X., Yan, C., Iyer, S., Rosendahl, I., Xu, Z., Rissanen, M. P., Riva, M., Taipale, R., Sarnela, N., Petäjä, T., Worsnop, D. R., Kulmala, M., Ehn, M., and Junninen, H.: The role of highly oxygenated molecules (HOMs) in determining the composition of ambient ions in the boreal forest, *Atmos. Chem. Phys.*, 17, 13819–13831, <https://doi.org/10.5194/acp-17-13819-2017>, 2017.
- Bianchi, F., Kurtén, T., Riva, M., Mohr, C., Rissanen, M. P., Roldin, P., Berndt, T., Crouse, J. D., Wennberg, P. O., Mentel, T. F., Wildt, J., Junninen, H., Jokinen, T., Kulmala, M., Worsnop, D. R., Thornton, J. A., Donahue, N., Kjaergaard, H. G., and Ehn, M.: Highly oxygenated organic molecules (HOM) from gas-phase autoxidation involving peroxy radicals: a key contributor to atmospheric aerosol, *Chem. Rev.*, 119, 3472–3509, <https://doi.org/10.1021/acs.chemrev.8b00395>, 2019.
- Boers, R., van Weele, M., van Meijgaard, E., Savenije, M., Siebesma, A. P., Bosveld, F., and Stammes, P.: Observations and projections of visibility and aerosol optical thickness (1956–2100) in the Netherlands: impacts of time-varying aerosol composition and hygroscopicity, *Environ. Res. Lett.*, 10, 015003, <https://doi.org/10.1088/1748-9326/10/1/015003>, 2015.
- Boyd, C. M., Sanchez, J., Xu, L., Eugene, A. J., Nah, T., Tuet, W. Y., Guzman, M. I., and Ng, N. L.: Secondary organic aerosol formation from the  $\beta$ -pinene + NO<sub>3</sub> system: effect of humidity and peroxy radical fate, *Atmos. Chem. Phys.*, 15, 7497–7522, <https://doi.org/10.5194/acp-15-7497-2015>, 2015.
- Caldwell, G. W., Masucci, J. A., and Ikononou, M. G.: Negative-ion chemical ionization mass-spectrometry binding of molecules to bromide and iodide Anions, *Org. Mass Spectrom.*, 24, 8–14, <https://doi.org/10.1002/oms.1210240103>, 1989.
- Cappa, C. D. and Jimenez, J. L.: Quantitative estimates of the volatility of ambient organic aerosol, *Atmos. Chem. Phys.*, 10, 5409–5424, <https://doi.org/10.5194/acp-10-5409-2010>, 2010.
- Daumit, K. E., Kessler, S. H., and Kroll, J. H.: Average chemical properties and potential formation pathways of highly oxidized organic aerosol, *Faraday Discuss.*, 165, 181–202, <https://doi.org/10.1039/C3FD00045A>, 2013.
- Donahue, N. M., Robinson, A. L., Stanier, C. O., and Pandis, S. N.: Coupled partitioning, dilution, and chemical aging of semivolatile organics, *Environ. Sci. Technol.*, 40, 2635–2643, <https://doi.org/10.1021/es052297c>, 2006.
- Donahue, N. M., Robinson, A. L., and Pandis, S. N.: Atmospheric organic particulate matter: from smoke to secondary organic aerosol, *Atmos. Environ.*, 43, 94–106, <https://doi.org/10.1016/j.atmosenv.2008.09.055>, 2009.
- Donahue, N. M., Epstein, S. A., Pandis, S. N., and Robinson, A. L.: A two-dimensional volatility basis set: 1. organic-aerosol mixing thermodynamics, *Atmos. Chem. Phys.*, 11, 3303–3318, <https://doi.org/10.5194/acp-11-3303-2011>, 2011.
- Donahue, N. M., Kroll, J. H., Pandis, S. N., and Robinson, A. L.: A two-dimensional volatility basis set – Part 2: Diagnostics of organic-aerosol evolution, *Atmos. Chem. Phys.*, 12, 615–634, <https://doi.org/10.5194/acp-12-615-2012>, 2012.
- Ehn, M., Thornton, J. A., Kleist, E., Sipilä, M., Junninen, H., Pullinen, I., Springer, M., Rubach, F., Tillmann, R., Lee, B.,

- Lopez-Hilfiker, F., Andres, S., Acir, I. H., Rissanen, M., Jokinen, T., Schobesberger, S., Kangasluoma, J., Kontkanen, J., Nieminen, T., Kurtén, T., Nielsen, L. B., Jørgensen, S., Kjaergaard, H. G., Canagaratna, M., Dal Maso, M., Berndt, T., Petäjä, T., Wahner, A., Kerminen, V. M., Kulmala, M., Worsnop, D. R., Wildt, J., and Mentel, T. F.: A large source of low-volatility secondary organic aerosol, *Nature*, 506, 476–479, <https://doi.org/10.1038/nature13032>, 2014.
- Epstein, S. A., Riipinen, I., and Donahue, N. M.: A semiempirical correlation between enthalpy of vaporization and saturation concentration for organic aerosol, *Environ. Sci. Technol.*, 44, 743–748, <https://doi.org/10.1021/es902497z>, 2010.
- Faxon, C., Hammes, J., Le Breton, M., Pathak, R. K., and Hallquist, M.: Characterization of organic nitrate constituents of secondary organic aerosol (SOA) from nitrate-radical-initiated oxidation of limonene using high-resolution chemical ionization mass spectrometry, *Atmos. Chem. Phys.*, 18, 5467–5481, <https://doi.org/10.5194/acp-18-5467-2018>, 2018.
- Gross, J. H.: *Mass Spectrometry*, 3rd edn., Springer International Publishing, Cham, Switzerland, 2017.
- Guenther, A., Hewitt, C. N., Erickson, D., Fall, R., Geron, C., Graedel, T., Harley, P., Klinger, L., Lerdau, M., McKay, W. A., Pierce, T., Scholes, B., Steinbrecher, R., Tallamraju, R., Taylor, J., and Zimmerman, P.: A global model of natural volatile organic compound emissions, *J. Geophys. Res.-Atmos.*, 100, 8873–8892, <https://doi.org/10.1029/94jd02950>, 1995.
- Hakola, H., Hellén, H., Hemmilä, M., Rinne, J., and Kulmala, M.: In situ measurements of volatile organic compounds in a boreal forest, *Atmos. Chem. Phys.*, 12, 11665–11678, <https://doi.org/10.5194/acp-12-11665-2012>, 2012.
- Hammes, J., Lutz, A., Mentel, T., Faxon, C., and Hallquist, M.: Carboxylic acids from limonene oxidation by ozone and hydroxyl radicals: insights into mechanisms derived using a FIGAERO-CIMS, *Atmos. Chem. Phys.*, 19, 13037–13052, <https://doi.org/10.5194/acp-19-13037-2019>, 2019.
- Hari, P. and Kulmala, M.: Station for measuring ecosystem-atmosphere relations, *Boreal Environ. Res.*, 10, 315–322, 2005.
- Heald, C. L., Henze, D. K., Horowitz, L. W., Feddes, J., Lamarque, J.-F., Guenther, A., Hess, P. G., Vitt, F., Seinfeld, J. H., Goldstein, A. H., and Fung, I.: Predicted change in global secondary organic aerosol concentrations in response to future climate, emissions, and land use change, *J. Geophys. Res.-Atmos.*, 113, D05211, <https://doi.org/10.1029/2007JD009092>, 2008.
- Heikkinen, L., Äijälä, M., Riva, M., Luoma, K., Dällenbach, K., Aalto, J., Aalto, P., Aliaga, D., Aurela, M., Keskinen, H., Makkonen, U., Rantala, P., Kulmala, M., Petäjä, T., Worsnop, D., and Ehn, M.: Long-term sub-micrometer aerosol chemical composition in the boreal forest: inter- and intra-annual variability, *Atmos. Chem. Phys.*, 20, 3151–3180, <https://doi.org/10.5194/acp-20-3151-2020>, 2020.
- Heinritzi, M., Simon, M., Steiner, G., Wagner, A. C., Kürten, A., Hansel, A., and Curtius, J.: Characterization of the mass-dependent transmission efficiency of a CIMS, *Atmos. Meas. Tech.*, 9, 1449–1460, <https://doi.org/10.5194/amt-9-1449-2016>, 2016.
- Huang, W.: Data for “Measurement report: Molecular composition and volatility of gaseous organic compounds in a boreal forest – from volatile organic compounds to highly oxygenated organic molecules”, Zenodo [data set], <https://doi.org/10.5281/zenodo.4925730>, 2021.
- Huang, W., Saathoff, H., Shen, X., Ramisetty, R., Leisner, T., and Mohr, C.: Chemical characterization of highly functionalized organonitrates contributing to night-time organic aerosol mass loadings and particle growth, *Environ. Sci. Technol.*, 53, 1165–1174, <https://doi.org/10.1021/acs.est.8b05826>, 2019a.
- Huang, W., Saathoff, H., Shen, X., Ramisetty, R., Leisner, T., and Mohr, C.: Seasonal characteristics of organic aerosol chemical composition and volatility in Stuttgart, Germany, *Atmos. Chem. Phys.*, 19, 11687–11700, <https://doi.org/10.5194/acp-19-11687-2019>, 2019b.
- Hyttinen, N., Otkjaer, R. V., Iyer, S., Kjaergaard, H. G., Rissanen, M. P., Wennberg, P. O., and Kurtén, T.: Computational comparison of different reagent ions in the chemical ionization of oxidized multifunctional compounds, *J. Phys. Chem. A*, 122, 269–279, <https://doi.org/10.1021/acs.jpca.7b10015>, 2018.
- IPCC: *Climate change 2013: The physical scientific basis*, edited by: Stocker, T. F., Qin, D., Plattner, G.-K., Tignor, M., Allen, S. K., Boschung, J., Nauels, A., Xia, Y., Bex, V., and Midgley, P. M., Cambridge University Press, Cambridge, UK, 622–623, 2013.
- Isaacman-VanWertz, G. and Aumont, B.: Impact of organic molecular structure on the estimation of atmospherically relevant physicochemical parameters, *Atmos. Chem. Phys.*, 21, 6541–6563, <https://doi.org/10.5194/acp-21-6541-2021>, 2021.
- Junninen, H., Ehn, M., Petäjä, T., Luosujärvi, L., Kotiaho, T., Koskinen, R., Rohner, U., Gonin, M., Fuhrer, K., Kulmala, M., and Worsnop, D. R.: A high-resolution mass spectrometer to measure atmospheric ion composition, *Atmos. Meas. Tech.*, 3, 1039–1053, <https://doi.org/10.5194/amt-3-1039-2010>, 2010.
- Kaser, L., Karl, T., Guenther, A., Graus, M., Schnitzhofer, R., Turnipseed, A., Fischer, L., Harley, P., Madronich, M., Gochis, D., Keutsch, F. N., and Hansel, A.: Undisturbed and disturbed above canopy ponderosa pine emissions: PTR-TOF-MS measurements and MEGAN 2.1 model results, *Atmos. Chem. Phys.*, 13, 11935–11947, <https://doi.org/10.5194/acp-13-11935-2013>, 2013.
- Kirkby, J., Duplissy, J., Sengupta, K., Frege, C., Gordon, H., Williamson, C., Heinritzi, M., Simon, M., Yan, C., Almeida, J., Tröstl, J., Nieminen, T., Ortega, I. K., Wagner, R., Adamov, A., Amorim, A., Bernhammer, A.-K., Bianchi, F., Breitenlechner, M., Brilke, S., Chen, X. M., Craven, J., Dias, A., Ehrhart, S., Flanagan, R. C., Franchin, A., Fuchs, C., Guida, R., Hakala, J., Hoyle, C. R., Jokinen, T., Junninen, H., Kangasluoma, J., Kim, J., Krapf, M., Kürten, A., Laaksonen, A., Lehtipalo, K., Makhmutov, V., Mathot, S., Molteni, U., Onnela, A., Peräkylä, O., Piel, F., Petäjä, T., Praplan, A. P., Pringle, K., Rap, A., Richards, N. A. D., Riipinen, I., Rissanen, M. P., Rondo, L., Sarnela, N., Schobesberger, S., Scott, C. E., Seinfeld, J. H., Sipilä, M., Steiner, G., Stozhkov, Y., Stratmann, F., Tomé, A., Virtanen, A., Vogel, A. L., Wagner, A. C., Wagner, P. E., Weingartner, E., Wimmer, D., Winkler, P. M., Ye, P. L., Zhang, X., Hansel, A., Dommen, J., Donahue, N. M., Worsnop, D. R., Baltensperger, U., Kulmala, M., Carslaw, K. S., and Curtius, J.: Ion-induced nucleation of pure biogenic particles, *Nature*, 533, 521–526, <https://doi.org/10.1038/nature17953>, 2016.
- Krechmer, J., Lopez-Hilfiker, F., Koss, A., Hutterli, M., Stoermer, C., Deming, B., Kimmel, J., Warneke, C., Holzinger, R., Jayne, J., Worsnop, D., Fuhrer, K., Gonin, M., and

- de Gouw, J.: Evaluation of a new reagent-ion source and focusing ion-molecule reactor for use in proton-transfer-reaction mass spectrometry, *Anal. Chem.*, 90, 12011–12018, <https://doi.org/10.1021/acs.analchem.8b02641>, 2018.
- Kulmala, M., Toivonen, A., Mäkelä, J. M., and Laaksonen, A.: Analysis of the growth of nucleation mode particles observed in boreal forest, *Tellus B*, 50, 449–462, <https://doi.org/10.3402/tellusb.v50i5.16229>, 1998.
- Kulmala, M., Kontkanen, J., Junninen, H., Lehtipalo, K., Manninen, H. E., Nieminen, T., Petäjä, T., Sipilä, M., Schobesberger, S., Rantala, P., Franchin, A., Jokinen, T., Järvinen, E., Äijälä, M., Kangasluoma, J., Hakala, J., Aalto, P. P., Paasonen, P., Mikkilä, J., Vanhanen, J., Aalto, J., Hakola, H., Makkonen, U., Ruuskanen, T., Mauldin III, R. L., Duplissy, J., Vehkamäki, H., Bäck, J., Kortelainen, A., Riipinen, I., Kurtén, T., Johnston, M. V., Smith, J. N., Ehn, M., Mentel, T. F., Lehtinen, K. E. J., Laaksonen, A., Kerminen, V.-M., and Worsnop, D. R.: Direct observations of atmospheric aerosol nucleation, *Science*, 339, 943–946, <https://doi.org/10.1126/science.1227385>, 2013.
- Kürten, A., Rondo, L., Ehrhart, S., and Curtius, J.: Calibration of a chemical ionization mass spectrometer for the measurement of gaseous sulfuric acid, *J. Phys. Chem. A*, 116, 6375–6386, <https://doi.org/10.1021/jp212123n>, 2012.
- Lee, B. H., Mohr, C., Lopez-Hilfiker, F. D., Lutz, A., Hallquist, M., Lee, L., Romer, P., Cohen, R. C., Iyer, S., Kurtén, T., Hu, W. W., Day, D. A., Campuzano-Jost, P., Jimenez, J. L., Xu, L., Ng, N. L., Guo, H. Y., Weber, R. J., Wild, R. J., Brown, S. S., Koss, A., de Gouw, J., Olson, K., Goldstein, A. H., Seco, R., Kim, S., McAvey, K., Shepson, P. B., Starn, T., Baumann, K., Edgerton, E. S., Liu, J. M., Shilling, J. E., Miller, D. O., Brune, W., Schobesberger, S., D'Ambro, E. L., and Thornton, J. A.: Highly functionalized organic nitrates in the southeast United States: Contribution to secondary organic aerosol and reactive nitrogen budgets, *P. Natl. Acad. Sci. USA*, 113, 1516–1521, <https://doi.org/10.1073/pnas.1508108113>, 2016.
- Li, H., Riva, M., Rantala, P., Heikkinen, L., Daellenbach, K., Krechmer, J. E., Flaud, P.-M., Worsnop, D., Kulmala, M., Villenave, E., Perraudin, E., Ehn, M., and Bianchi, F.: Terpenes and their oxidation products in the French Landes forest: insights from Vocus PTR-TOF measurements, *Atmos. Chem. Phys.*, 20, 1941–1959, <https://doi.org/10.5194/acp-20-1941-2020>, 2020.
- Li, H., Canagaratna, M. R., Riva, M., Rantala, P., Zhang, Y., Thomas, S., Heikkinen, L., Flaud, P.-M., Villenave, E., Perraudin, E., Worsnop, D., Kulmala, M., Ehn, M., and Bianchi, F.: Atmospheric organic vapors in two European pine forests measured by a Vocus PTR-TOF: insights into monoterpene and sesquiterpene oxidation processes, *Atmos. Chem. Phys.*, 21, 4123–4147, <https://doi.org/10.5194/acp-21-4123-2021>, 2021.
- Li, Y., Pöschl, U., and Shiraiwa, M.: Molecular corridors and parameterizations of volatility in the chemical evolution of organic aerosols, *Atmos. Chem. Phys.*, 16, 3327–3344, <https://doi.org/10.5194/acp-16-3327-2016>, 2016.
- Liao, L., Dal Maso, M., Taipale, R., Rinne, J., Ehn, M., Junninen, H., Äijälä, M., Nieminen, T., Alekseychik, P., Hultkonen, M., Worsnop, D. R., Kerminen, V.-M., and Kulmala, M.: Monoterpene pollution episodes in a forest environment: indication of anthropogenic origin and association with aerosol particles, *Boreal Environ. Res.*, 16, 288–303, 2011.
- Lopez-Hilfiker, F. D., Mohr, C., Ehn, M., Rubach, F., Kleist, E., Wildt, J., Mentel, Th. F., Lutz, A., Hallquist, M., Worsnop, D., and Thornton, J. A.: A novel method for online analysis of gas and particle composition: description and evaluation of a Filter Inlet for Gases and AEROSols (FIGAERO), *Atmos. Meas. Tech.*, 7, 983–1001, <https://doi.org/10.5194/amt-7-983-2014>, 2014.
- Manninen, H. E., Nieminen, T., Asmi, E., Gagné, S., Häkkinen, S., Lehtipalo, K., Aalto, P., Vana, M., Mirme, A., Mirme, S., Hörrak, U., Plass-Dülmer, C., Stange, G., Kiss, G., Hoffer, A., Törö, N., Moerman, M., Henzing, B., de Leeuw, G., Brinkenberg, M., Kouvarakis, G. N., Bougiatioti, A., Mihalopoulos, N., O'Dowd, C., Ceburnis, D., Arneth, A., Svenningsson, B., Swietlicki, E., Tarozzi, L., Decesari, S., Facchini, M. C., Birmili, W., Sonntag, A., Wiedensohler, A., Boulon, J., Sellegri, K., Laj, P., Gysel, M., Bukowiecki, N., Weingartner, E., Wehrle, G., Laaksonen, A., Hamed, A., Joutsensaari, J., Petäjä, T., Kerminen, V.-M., and Kulmala, M.: EUCAARI ion spectrometer measurements at 12 European sites – analysis of new particle formation events, *Atmos. Chem. Phys.*, 10, 7907–7927, <https://doi.org/10.5194/acp-10-7907-2010>, 2010.
- Massoli, P., Stark, H., Canagaratna, M. R., Krechmer, J. E., Xu, L., Ng, N. L., Mauldin, R. L., Yan, C., Kimmel, J., Misztal, P. K., Jimenez, J. L., Jayne, J. T., and Worsnop, D. R.: Ambient measurements of highly oxidized gas-phase molecules during the Southern Oxidant and Aerosol Study (SOAS) 2013, *ACS Earth Space Chem.*, 2, 653–672, <https://doi.org/10.1021/acsearthspacechem.8b00028>, 2018.
- Mohr, C., Thornton, J. A., Heitto, A., Lopez-Hilfiker, F. D., Lutz, A., Riipinen, I., Hong, J., Donahue, N. M., Hallquist, M., Petaja, T., Kulmala, M., and Yli-Juuti, T.: Molecular identification of organic vapors driving atmospheric nanoparticle growth, *Nat. Commun.*, 10, 4442, <https://doi.org/10.1038/s41467-019-12473-2>, 2019.
- Molteni, U., Simon, M., Heinritzi, M., Hoyle, C. R., Bernhammer, A.-K., Bianchi, F., Breitenlechner, M., Brilke, S., Dias, A., Duplissy, J., Frege, C., Gordon, H., Heyn, C., Jokinen, T., Kürten, A., Lehtipalo, K., Makhmutov, V., Petäjä, T., Pieber, S. M., Praplan, A. P., Schobesberger, S., Steiner, G., Stozhkov, Y., Tomé, A., Tröstl, J., Wagner, A. C., Wagner, R., Williamson, C., Yan, C., Baltensperger, U., Curtius, J., Donahue, N. M., Hansel, A., Kirkby, J., Kulmala, M., Worsnop, D. R., and Dommen, J.: Formation of highly oxygenated organic molecules from  $\alpha$ -pinene ozonolysis: chemical characteristics, mechanism, and kinetic model development, *ACS Earth Space Chem.*, 3, 873–883, <https://doi.org/10.1021/acsearthspacechem.9b00035>, 2019.
- Nash, D. G., Baer, T., and Johnston, M. V.: Aerosol mass spectrometry: an introductory review, *Int. J. Mass Spectrom.*, 258, 2–12, <https://doi.org/10.1016/j.ijms.2006.09.017>, 2006.
- Nel, A.: Air pollution-related illness: effects of particles, *Science*, 308, 804–806, <https://doi.org/10.1126/science.1108752>, 2005.
- Ng, N. L., Herndon, S. C., Trimborn, A., Canagaratna, M. R., Croteau, P. L., Onasch, T. B., Sueper, D., Worsnop, D. R., Zhang, Q., Sun, Y. L., and Jayne, J. T.: An aerosol chemical speciation monitor (ACSM) for routine monitoring of the composition and mass concentrations of ambient aerosol, *Aerosol Sci. Tech.*, 45, 780–794, <https://doi.org/10.1080/02786826.2011.560211>, 2011.
- Pankow, J. F. and Asher, W. E.: SIMPOL.1: a simple group contribution method for predicting vapor pressures and enthalpies of vaporization of multifunctional organic compounds, *Atmos.*

- Chem. Phys., 8, 2773–2796, <https://doi.org/10.5194/acp-8-2773-2008>, 2008.
- Rissanen, M. P., Mikkilä, J., Iyer, S., and Hakala, J.: Multi-scheme chemical ionization inlet (MION) for fast switching of reagent ion chemistry in atmospheric pressure chemical ionization mass spectrometry (CIMS) applications, *Atmos. Meas. Tech.*, 12, 6635–6646, <https://doi.org/10.5194/amt-12-6635-2019>, 2019.
- Riva, M., Rantala, P., Krechmer, J. E., Peräkylä, O., Zhang, Y., Heikkinen, L., Garmash, O., Yan, C., Kulmala, M., Worsnop, D., and Ehn, M.: Evaluating the performance of five different chemical ionization techniques for detecting gaseous oxygenated organic species, *Atmos. Meas. Tech.*, 12, 2403–2421, <https://doi.org/10.5194/amt-12-2403-2019>, 2019.
- Rückerl, R., Schneider, A., Breitner, S., Cyruss, J., and Peters, A.: Health effects of particulate air pollution: a review of epidemiological evidence, *Inhal. Toxicol.*, 23, 555–592, <https://doi.org/10.3109/08958378.2011.593587>, 2011.
- Sanchez, J., Tanner, D. J., Chen, D., Huey, L. G., and Ng, N. L.: A new technique for the direct detection of HO<sub>2</sub> radicals using bromide chemical ionization mass spectrometry (Br-CIMS): initial characterization, *Atmos. Meas. Tech.*, 9, 3851–3861, <https://doi.org/10.5194/amt-9-3851-2016>, 2016.
- Schervish, M. and Donahue, N. M.: Peroxy radical chemistry and the volatility basis set, *Atmos. Chem. Phys.*, 20, 1183–1199, <https://doi.org/10.5194/acp-20-1183-2020>, 2020.
- Sekimoto, K., Li, S. M., Yuan, B., Koss, A., Coggon, M., Warneke, C., and de Gouw, J.: Calculation of the sensitivity of proton-transfer-reaction mass spectrometry (PTR-MS) for organic trace gases using molecular properties, *Int. J. Mass Spectrom.*, 421, 71–94, <https://doi.org/10.1016/j.ijms.2017.04.006>, 2017.
- Simon, M., Dada, L., Heinritzi, M., Scholz, W., Stolzenburg, D., Fischer, L., Wagner, A. C., Kürten, A., Rörup, B., He, X.-C., Almeida, J., Baalbaki, R., Baccarini, A., Bauer, P. S., Beck, L., Bergen, A., Bianchi, F., Bräkling, S., Brilke, S., Caudillo, L., Chen, D., Chu, B., Dias, A., Draper, D. C., Duplissy, J., El-Haddad, I., Finkenzeller, H., Frege, C., Gonzalez-Carracedo, L., Gordon, H., Granzin, M., Hakala, J., Hofbauer, V., Hoyle, C. R., Kim, C., Kong, W., Lamkaddam, H., Lee, C. P., Lehtipalo, K., Leiminger, M., Mai, H., Manninen, H. E., Marie, G., Marten, R., Mentler, B., Molteni, U., Nichman, L., Nie, W., Ojdanic, A., Onnela, A., Partoll, E., Petäjä, T., Pfeifer, J., Philipov, M., Quéléver, L. L. J., Ranjithkumar, A., Rissanen, M. P., Schallhart, S., Schobesberger, S., Schuchmann, S., Shen, J., Sipilä, M., Steiner, G., Stozhkov, Y., Tauber, C., Tham, Y. J., Tomé, A. R., Vazquez-Pufleau, M., Vogel, A. L., Wagner, R., Wang, M., Wang, D. S., Wang, Y., Weber, S. K., Wu, Y., Xiao, M., Yan, C., Ye, P., Ye, Q., Zauner-Wieczorek, M., Zhou, X., Baltensperger, U., Dommen, J., Flagan, R. C., Hansel, A., Kulmala, M., Volkamer, R., Winkler, P. M., Worsnop, D. R., Donahue, N. M., Kirkby, J., and Curtius, J.: Molecular understanding of new-particle formation from  $\alpha$ -pinene between  $-50$  and  $+25$  °C, *Atmos. Chem. Phys.*, 20, 9183–9207, <https://doi.org/10.5194/acp-20-9183-2020>, 2020.
- Sindelarova, K., Granier, C., Bouarar, I., Guenther, A., Tilmes, S., Stavrou, T., Müller, J.-F., Kuhn, U., Stefani, P., and Knorr, W.: Global data set of biogenic VOC emissions calculated by the MEGAN model over the last 30 years, *Atmos. Chem. Phys.*, 14, 9317–9341, <https://doi.org/10.5194/acp-14-9317-2014>, 2014.
- Stolzenburg, D., Fischer, L., Vogel, A. L., Heinritzi, M., Schervish, M., Simon, M., Wagner, A. C., Dada, L., Ahonen, L. R., Amorim, A., Baccarini, A., Bauer, P. S., Baumgartner, B., Bergen, A., Bianchi, F., Breitenlechner, M., Brilke, S., Mazon, S. B., Chen, D. X., Dias, A., Draper, D. C., Duplissy, J., Haddad, I., Finkenzeller, H., Frege, C., Fuchs, C., Garmash, O., Gordon, H., He, X., Helm, J., Hofbauer, V., Hoyle, C. R., Kim, C., Kirkby, J., Kontkanen, J., Kürten, A., Lampilahti, J., Lawler, M., Lehtipalo, K., Leiminger, M., Mai, H., Mathot, S., Mentler, B., Molteni, U., Nie, W., Nieminen, T., Nowak, J. B., Ojdanic, A., Onnela, A., Passananti, M., Petäjä, T., Quéléver, L. L. J., Rissanen, M. P., Sarnela, N., Schallhart, S., Tauber, C., Tomé, A., Wagner, R., Wang, M., Weitz, L., Wimmer, D., Xiao, M., Yan, C., Ye, P., Zha, Q., Baltensperger, U., Curtius, J., Dommen, J., Flagan, R. C., Kulmala, M., Smith, J. N., Worsnop, D. R., Hansel, A., Donahue, N. M., and Winkler, P. M.: Rapid growth of organic aerosol nanoparticles over a wide tropospheric temperature range, *P. Natl. Acad. Sci. USA*, 115, 9122–9127, <https://doi.org/10.1073/pnas.1807604115>, 2018.
- Sullivan, R. C. and Prather, K. A.: Recent advances in our understanding of atmospheric chemistry and climate made possible by on-line aerosol analysis instrumentation, *Anal. Chem.*, 77, 3861–3885, <https://doi.org/10.1021/ac050716i>, 2005.
- Tröstl, J., Chuang, W. K., Gordon, H., Heinritzi, M., Yan, C., Molteni, U., Ahlm, L., Frege, C., Bianchi, F., Wagner, R., Simon, M., Lehtipalo, K., Williamson, C., Craven, J. S., Duplissy, J., Adamov, A., Almeida, J., Bernhammer, A.-K., Breitenlechner, M., Brilke, S., Dias, A., Ehrhart, S., Flagan, R. C., Franchin, A., Fuchs, C., Guida, R., Gysel, M., Hansel, A., Hoyle, C. R., Jokinen, T., Junninen, H., Kangasluoma, J., Keskinen, H., Kim, J., Krapf, M., Kürten, A., Laaksonen, A., Lawler, M., Leiminger, M., Mathot, S., Möhler, O., Nieminen, T., Onnela, A., Petäjä, T., Piel, F. M., Miettinen, P., Rissanen, M. P., Rondo, L., Sarnela, N., Schobesberger, S., Sengupta, K., Sipilä, M., Smith, J. N., Steiner, G., Tomé, A., Virtanen, A., Wagner, A. C., Weingartner, E., Wimmer, D., Winkler, P. M., Ye, P. L., Carslaw, K. S., Curtius, J., Dommen, J., Kirkby, J., Kulmala, M., Riipinen, I., Worsnop, D. R., Donahue, N. M., and Baltensperger, U.: The role of low-volatility organic compounds in initial particle growth in the atmosphere, *Nature*, 533, 527–531, <https://doi.org/10.1038/nature18271>, 2016.
- Viggiano, A. A., Seeley, J. V., Mundis, P. L., Williamson, J. S., and Morris, R. A.: Rate constants for the reactions of XO<sub>3</sub>–(H<sub>2</sub>O)(*n*) (*X* = C, HC, and N) and NO<sub>3</sub>–(HNO<sub>3</sub>)(*n*) with H<sub>2</sub>SO<sub>4</sub>: implications for atmospheric detection of H<sub>2</sub>SO<sub>4</sub>, *J. Phys. Chem. A*, 101, 8275–8278, <https://doi.org/10.1021/jp971768h>, 1997.
- Wang, M. Y., Chen, D. X., Xiao, M., Ye, Q., Stolzenburg, D., Hofbauer, V., Ye, P. L., Vogel, A. L., Mauldin III, R. L., Amorim, A., Baccarini, A., Baumgartner, B., Brilke, S., Dada, L., Dias, A., Duplissy, J., Finkenzeller, H., Garmash, O., He, X. C., Hoyle, C. R., Kim, C., Kvashnin, A., Lehtipalo, K., Fischer, L., Molteni, U., Petäjä, T., Pospisilova, V., Quéléver, L. L. J., Rissanen, M., Simon, M., Tauber, C., Tomé, A., Wagner, A. C., Weitz, L., Volkamer, R., Winkler, P. M., Kirkby, J., Worsnop, D. R., Kulmala, M., Baltensperger, U., Dommen, J., El-Haddad, I., and Donahue, N. M.: Photo-oxidation of aromatic hydrocarbons produces low-volatility organic compounds, *Environ. Sci. Technol.*, 54, 7911–7921, <https://doi.org/10.1021/acs.est.0c02100>, 2020.

- Williams, J., Crowley, J., Fischer, H., Harder, H., Martinez, M., Petäjä, T., Rinne, J., Bäck, J., Boy, M., Dal Maso, M., Hakala, J., Kajos, M., Keronen, P., Rantala, P., Aalto, J., Aaltonen, H., Paatero, J., Vesala, T., Hakola, H., Levula, J., Pohja, T., Herrmann, F., Auld, J., Mesarchaki, E., Song, W., Yassaa, N., Nölscher, A., Johnson, A. M., Custer, T., Sinha, V., Thieser, J., Povesle, N., Taraborrelli, D., Tang, M. J., Bozem, H., Hosaynali-Beygi, Z., Axinte, R., Oswald, R., Novelli, A., Kubistin, D., Hens, K., Javed, U., Trawny, K., Breitenberger, C., Hidalgo, P. J., Ebben, C. J., Geiger, F. M., Corrigan, A. L., Russell, L. M., Ouwersloot, H. G., Vilà-Guerau de Arellano, J., Ganzeveld, L., Vogel, A., Beck, M., Bayerle, A., Kampf, C. J., Bertelmann, M., Köllner, F., Hoffmann, T., Valverde, J., González, D., Riekkola, M.-L., Kulmala, M., and Lelieveld, J.: The summertime Boreal forest field measurement intensive (HUMPPA-COPEC-2010): an overview of meteorological and chemical influences, *Atmos. Chem. Phys.*, 11, 10599–10618, <https://doi.org/10.5194/acp-11-10599-2011>, 2011.
- Yan, C., Nie, W., Äijälä, M., Rissanen, M. P., Canagaratna, M. R., Massoli, P., Junninen, H., Jokinen, T., Sarnela, N., Häme, S. A. K., Schobesberger, S., Canonaco, F., Yao, L., Prévôt, A. S. H., Petäjä, T., Kulmala, M., Sipilä, M., Worsnop, D. R., and Ehn, M.: Source characterization of highly oxidized multifunctional compounds in a boreal forest environment using positive matrix factorization, *Atmos. Chem. Phys.*, 16, 12715–12731, <https://doi.org/10.5194/acp-16-12715-2016>, 2016.
- Ye, Q., Wang, M. Y., Hofbauer, V., Stolzenburg, D., Chen, D. X., Schervish, M., Vogel, A., Mauldin, R. L., Baalbaki, R., Brilke, S., Dada, L., Dias, A., Duplissy, J., El Haddad, I., Finkenzeller, H., Fischer, L., He, X. C., Kim, C., Kürten, A., Lamkaddam, H., Lee, C. P., Lehtipalo, K., Leiminger, M., Manninen, H. E., Marten, R., Mentler, B., Partoll, E., Petäjä, T., Rissanen, M., Schobesberger, S., Schuchmann, S., Simon, M., Tham, Y. J., Vazquez-Pufleau, M., Wagner, A. C., Wang, Y. H., Wu, Y. S., Xiao, M., Baltensperger, U., Curtius, J., Flagan, R., Kirkby, J., Kulmala, M., Volkamer, R., Winkler, P. M., Worsnop, D., and Donahue, N. M.: Molecular composition and volatility of nucleated particles from alpha-pinene oxidation between  $-50^{\circ}\text{C}$  and  $+25^{\circ}\text{C}$ , *Environ. Sci. Technol.*, 53, 12357–12365, <https://doi.org/10.1021/acs.est.9b03265>, 2019.
- Yuan, B., Koss, A. R., Warneke, C., Coggon, M., Sekimoto, K., and de Gouw, J. A.: Proton-transfer-reaction mass spectrometry: applications in atmospheric sciences, *Chem. Rev.*, 117, 13187–13229, <https://doi.org/10.1021/acs.chemrev.7b00325>, 2017.
- Zha, Q., Yan, C., Junninen, H., Riva, M., Sarnela, N., Aalto, J., Quéléver, L., Schallhart, S., Dada, L., Heikkinen, L., Peräkylä, O., Zou, J., Rose, C., Wang, Y., Mammarella, I., Katul, G., Vesala, T., Worsnop, D. R., Kulmala, M., Petäjä, T., Bianchi, F., and Ehn, M.: Vertical characterization of highly oxygenated molecules (HOMs) below and above a boreal forest canopy, *Atmos. Chem. Phys.*, 18, 17437–17450, <https://doi.org/10.5194/acp-18-17437-2018>, 2018.
- Zhang, X., McVay, R. C., Huang, D. D., Dalleska, N. F., Aumont, B., Flagan, R. C., and Seinfeld, J. H.: Formation and evolution of molecular products in  $\alpha$ -pinene secondary organic aerosol, *P. Natl. Acad. Sci. USA*, 112, 14168–14173, <https://doi.org/10.1073/pnas.1517742112>, 2015.
- Zhang, X., Lambe, A. T., Upshur, M. A., Brooks, W. A., Beì, A. G., Thomson, R. J., Geiger, F. M., Surratt, J. D., Zhang, Z. F., Gold, A., Graf, S., Cubison, M. J., Groessler, M., Jayne, J. T., Worsnop, D. R., and Canagaratna, M. R.: Highly oxygenated multifunctional compounds in  $\alpha$ -pinene secondary organic aerosol, *Environ. Sci. Technol.*, 51, 5932–5940, <https://doi.org/10.1021/acs.est.6b06588>, 2017.
- Zhao, Y., Thornton, J. A., and Pye, H. O. T.: Quantitative constraints on autoxidation and dimer formation from direct probing of monoterpene-derived peroxy radical chemistry, *P. Natl. Acad. Sci. USA*, 115, 12142–12147, <https://doi.org/10.1073/pnas.1812147115>, 2018.